SUPPLEMENTARY MATERIAL

Phytochemical analysis of areal part of *Ikonnikovia kaufmanniana* and their protection of DNA damage

Aizhamal Baiseitova, Janar Jenis, Jeong Yoon Kim, Zuo Peng Li and Ki Hun Park*

Division of Applied Life Science (BK21 plus), IALS, Gyeongsang National University, Jinju, 52828, Republic of Korea

***Correspondence to**:
Prof. Dr. Ki Hun Park, Division of Applied Life Science (BK21 plus), IALS,
Gyeongsang National University, Jinju 52828, Republic of Korea.
E-mail: khpark@gnu.ac.kr Phone: +82-55-772-1965 Fax +82-55-772-1969

Abstract

Ikonnikovia kaufmanniana is an endemic plant of Kazakhstan of which phytochemical analysis has not been reported. Present study found out that this species enriched with antioxidant chemicals. Isolation and structural identification processes gave twelve phenolic compounds (**1**-**12**) having dihydroflavanonol, flavonol, isoflavone and flavanol skeletons. The annotation of individual components in the extract was carried out by LC-ESI-MS/MS to represent a chemotaxonomic marker of the target plant. All compounds antioxidant activities were screened using three different radical sources (DPPH, ORAC, and hydroxyl radicals). Most compounds (**1**-**11**) had significant antioxidant activity against three radical sources, and their efficacies were revealed to differ by their functionality and skeleton. The potential of the isolated compounds in preventing oxidative damage of DNA was evaluated with pBR322 plasmid DNA. Compounds (**1**, **5**, **7**, and **8**) had protective effects on DNA damaged with 80% efficacy at 60 μM concentration.

Keywords: *Ikonnikovia kaufmanniana*; antioxidant activity; phytochemical composition; DNA damage protection.

Experimental section

Instruments

NMR spectra were recorded on a Bruker (AM 300, 500 MHz) spectrometer. Mass spectra were obtained on a JEOL JMS-700 (JEOL Ltd., Akishima, Japan). The MPLC and recycling HPLC was performed using a LC-Forte/R 100 (YMC Co., LTD, Kyoto, Japan) system equipped with a three channels UV detector. Fluorescence of ORAC was measured on a SpectraMaxM3 Multi-Mode Microplate Reader (Molecular device, USA). DPPH and hydroxyl radicals were measured using a JEOL JES-TE300 ESR spectrometer (JEOL Ltd., Akishima, Japan).

Chemicals and materials

Column chromatography was performed using MCI GEL CHP20P (Sigma Aldrich), Octadecylsilanized (ODS) silica gel (50 mm, YMC Ltd, Japan) and Sephadex LH-20 (50 mm, Amersham Pharmacia Biotech, Sweden). 2,2-Diphenyl-1-picrylhydrazyl (DPPH), 6-hydroxyl-2,5,7,8-tetramethylchroman-2-carboxylic acid (Trolox), 5,5-dimethyl-1-pyrroline *N*-oxide (DMPO), hydrogen peroxide (30%, H_2O_2), dimethyl sulfoxide (DMSO), 2,2′-azobis (2-methylpropionamidine) dihydrochloride (AAPH), fluorescein, were purchased from Sigma Aldrich (St. Louis, MO, USA). pBR322 plasmid DNA was purchased from Thermo Fisher Scientific (Waltham, MA, USA). All other chemicals were of analytical grade.

Plant material

The aerial part of *Ikonnikovia kaufmanniana* was collected during its flowering stage in June 2016 from the piedmont steppe of the Toraigir Mountains of Almaty region and identified by Dr. Alibek Ydyrys. Specimens (6349a) were deposited in the Herbarium of Laboratory Plant Biomorphology, Faculty of Biology and Biotechnology, Al-Farabi Kazakh National University,

Extraction and isolation

The air-dried *I. kaufmanniana* aerial (1.4 kg) was extracted with MeOH (30 L) at room temperature to give crude extract (143.6 g). Then, the crude extract was suspended in water and partionated into ethyl acetate to obtain ethyl acetate fraction (37.5 g). The ethyl acetate fraction (12 g) was subjected to column chromatography on MCI gel using water-methanol gradient (8:1 – 0:1) to obtain 10 fractions (A – J). Fractions A-F were rechromatographed separately using Sephadex LH-20 eluted with methanol, to give compounds **1** (28.5 mg), **2** (30.2 mg), **3** (40.6 mg), **5** (5.5 mg), **6** (20.6 mg), **7** (30.4 mg), **11** (7.9 mg) and **12** (18.1 mg). Fractions G and H, was performed on recycling HPLC using ODS gel column with water-methanol to afford compounds **8** (11.2 mg) and **9** (3.6 mg), respectively. Fractions I and J, was purified using Sephadex LH-20 eluted with chloroform-methanol (1:1), to give compounds **4** (15.8 mg) and **10** (3.8 mg), respectively.

Isolated compounds (**1**-**12**) were identified as dihydromyricetin potassium sulfate (**1**), gallocatechin (**2**), epigallocatechin (**3**), isoluteolin (**4**), myricetin (**5**), myricitrin (myricetin 3-O-α-L-rhamnopyranoside) (**6**), hyperoside (quercetin 3-O-β-D-galactoyranoside) (**7**), quercitrin (quercetin 3-O-α-L-rhamnopyranoside) (**8**), kaempferin (kaempferol 3-O-α-L-

rhamnopyranoside) (**9**), quercetin (**10**), dihydromyricetin (**11**), and rodiolinozide (**12**).

Compound **1** colourless needles; ^{1}H NMR (500 MHz, MeOD) δ 4.51 (1H, d, *J* = 11.6 Hz, H-3), 4.90 (1H, d, *J* = 11.6 Hz, H-2), 5.90 (1H, d, *J* = 2.0 Hz, H-6), 5.92 (1H, d, *J* = 2.0 Hz, H-8), 6.85 (1H, s, H-6'), 7.04 (2H, s, H-2'). ^{13}C NMR (125 MHz, MeOD) δ 73.7 (C-3), 84.9 (C-2), 96.3 (C-8), 97.4 (C-6), 101.9 (C-10), 113.5 (C-6'), 114.6 (C-2'), 129.1 (C-1'), 139.5 (C-4'), 141.6 (C-5'), 147.7 (C-3'), 164.4 (C-9), 162.3 (C-5), 168.7 (C-7), 192.3 (C-4). (Nonaka et al. 1983; Kim et al. 2014; Gadetskaya et al. 2015).

Compound **2** brown amorphous powder; EIMS, *m/z* 306 $[M]^+$; HREIMS, m/z 306.0745 $[M]^+$ (calcd for $C_{15}H_{14}O_7$ 306.0745); ^{1}H NMR (300 MHz, MeOD) δ 2.43 (1H, dd, *J* = 7.7, 16.2 Hz, H-4b), 2.74 (1H, dd, *J* = 5.3, 16.2 Hz, H-4a), 3.91 (1H, m, H-3), 4.49 (1H, d, *J* = 7.1 Hz, H-2), 5.83 (1H, d, *J* = 2.2 Hz, H-8), 5.89 (1H, d, *J* = 2.3 Hz, H-6), 6.37 (2H, s, H-2', H-6'). ^{13}C NMR (125 MHz, MeOD) δ 28.2 (C-4), 68.9 (C-3), 83.0 (C-2), 95.7 (C-8), 96.4 (C-6), 100.9 (C-10), 107.3 (C-2',6'), 131.7 (C-1'), 134.1 (C-4'), 147.0 (C-3', 5'), 157.0 (C-9), 157.7 (C-5), 157.9 (C-7) (Davis et al. 1996) .

Compound **3** brown amorphous powder; EIMS, *m/z* 306 $[M]^+$; HREIMS, m/z 306.0741 $[M]^+$ (calcd for $C_{15}H_{14}O_7$ 306.0745); ^{1}H NMR (300 MHz, MeOD) δ 2.66 (2H, m, H-4a, b), 4.13 (1H, m, H-3), 4.72 (1H, d, J = 2.0 Hz, H-2), 5.88 (1H, d, *J* = 2.3 Hz, H-8), 5.90 (1H, d, *J* = 2.3 Hz, H-6), 6.48 (1H, s, H-2'). ^{13}C NMR (125 MHz, MeOD) δ 29.2 (C-4), 67.6 (C-3), 80.0 (C-2), 96.0 (C-8), 96.5 (C-6), 100.3 (C-10), 107.2 (C-2', 6'), 131.7 (C-1′), 133.7 (C-4'), 146.8 (C-3', 5'), 157.5 (C-9), 157.8 (C-5), 158.1 (C-7) (Davis et al. 1996).

Compound **4** colorless amorphous powder; EIMS, *m/z* 286 $[M]^+$; ^{1}H NMR (500 MHz, MeOD) δ 6.16 (1H, d, *J* = 1.7, Hz, H-6) 6.28 (1H, d, *J* = 1.7 Hz, H-8), 6.77 (1H, d, *J* = 8.2 Hz, H-5'), 6.80 (1H, dd, *J* = 1.6, 8.2 Hz, H-6'), 6.98 (1H, d, *J* = 1.4 Hz, H-2'), 7.97 (1H, s, H-2). ^{13}C NMR (125 MHz, MeOD) δ 95.0 (C-8), 100.4 (C-6), 106.4 (C-10), 116.5 (C-5'), 117.6 (C-2'), 121.2 (C-6'), 124.0 (C-1′), 125.0 (C-3), 146.4 (C-4'), 147.0 (C-3'), 155.0 (C-2), 159.8 (C-5), 164.0 (C-9), 166.3 (C-7), 182.4 (C-4) (Fanie et al. 1980; Matsuda et al. 2004).

Compound **5** yellow amorphous powder; EIMS, *m/z* 318.0378 $[M]^+$; HREIMS, *m/z* 318.0378 $[M+H]^+$ (calcd for $C_{15}H_{10}O_8$ 318.0378); ^{1}H NMR (300 MHz, acetone-d_6) δ 6.26 (1H, d, *J* = 2.1 Hz, H-6), 6.51 (1H, d, *J* = 2.1 Hz, H-8), 7.42 (2H, s, H-2', H-6'). ^{13}C NMR (125 MHz, acetone-d_6) δ 94.5 (C-9), 99.2 (C-7), 104.2 (C-5), 108.4 (C-2', C-6'), 122.8 (C-1'), 136.5 (C-3), 137.0 (C-4'), 146.5 (C-3', C-5'), 147.1 (C-2), 157.8 (C-6), 162.4 (C-10), 165.0 (C-8), 176.6 (C-4) (David et al. 1996).

Compound **6** pale yellow amorphous powder; FABMS, *m/z* 465 $[M]^+$; HRFABMS, *m/z* 465.1061 $[M+H]^+$ (calcd for $C_{21}H_{20}O_{12}$ 465.1042); ^{1}H NMR (500 MHz, MeOD) δ 0.92 (3H, d, *J* = 6.25 Hz, H-6''), 3.27 (1H, m, H-5''), 3.48 (1H, m, H-4''), 3.745 (1H, m, H-3''), 4.18 (1H, m, H-2''), 5.28 (1H, d, *J* = 1.1 Hz, H-1''), 6.15 (1H, d, *J* = 1.2 Hz, H-6), 6.32 (1H, d, *J* = 1.9 Hz, H-8), 6.91 (2H, s, H-2', H-6'). ^{13}C NMR (125 MHz, MeOD) δ 94.7 (C-8), 100.0 (C-6), 106.1 (C-10), 109.8 (C-2', C-6'), 122.1 (C-1'), 136.5 (C-3), 138.1 (C-4'), 147.0 (C-3', C-5'), 158.7 (C-9), 159.6 (C-2), 163.4 (C-5),

166.0 (C-7), 179.8 (C-4), 17.9 (C-6"), 72.1 (C-2"), 72.2 (C-3"), 72.3 (C-5"), 73.5 (C-4"), 103.8 (C-1") (David et al. 1996).

Compound **7** yellow amorphous powder; FABMS, *m/z* 465 $[M]^+$; HRFABMS, *m/z* 465.1042 $[M+H]^+$ (calcd for $C_{21}H_{20}O_{12}$ 465.1042); ^{1}H NMR (300 MHz, DMSO–d_6) δ 3.17 - 3.65 (5H, m, H-2" to H-6"), 5.36 (1H, d, *J* = 7.7 Hz, H-1"), 6.18 (1H, d, *J* = 2.0, Hz, H-6) 6.38 (1H, d, *J* = 2.0 Hz, H-8), 6.81 (1H, d, *J* = 8.5 Hz, H-5'), 7.52 (1H, d, *J* = 2.2 Hz, H-2'), 7.64 (1H, dd, *J* = 2.2, 8.5 Hz, H-6'), 12.61 (1H, s, 5-OH). ^{13}C NMR (125 MHz, DMSO–d_6) δ 93.6 (C-8), 98.7 (C-6), 104.1 (C-10), 115.3 (C-5'), 116.1 (C-2'), 121.3 (C-1'), 122.1 (C-6'), 133.7 (C-3), 145.0 (C-3'), 148.6 (C-4'), 156.4 (C-2), 156.5 (C-9), 161.4 (C-5), 164.3 (C-7), 177.7 (C-4), 60.3 (C-6"), 68.9 (C-4"), 71.4 (C-2"), 73.3 (C-3"), 76.0 (C-5"), 102.8 (C-1") (Pereira 2012).

Compound **8** yellow amorphous powder; FABMS, *m/z* 447,36 $[M]^+$; ^{1}H NMR (300 MHz, MeOD) δ 0.93 (3H, d, *J* = 6.0, Hz, H-6"), 3.33 (1H, m, H-5"), 3.40 (1H, m, H-4"), 3.73 (1H, dd, *J* = 3.3, 9.2 Hz, H-3"), 4.21 (1H, dd, *J* = 1.6, 3.2 Hz, H-2"), 5.35 (1H, d, *J* = 1.5 Hz, H-1"), 6.20 (1H, d, *J* = 1.3, Hz, H-6), 6.36 (1H, d, *J* = 0.5 Hz, H-8), 6.90 (1H, d, *J* = 8.2 Hz, H-3'), 7.29 (1H, dd, *J* = 1.9, 8.3 Hz, H-6'), 7.32 (1H, d, *J* =2.0 Hz, H-2'). ^{13}C NMR (125 MHz, MeOD) δ 94.9 (C-8), 100.1 (C-6), 106.0 (C-10), 116.6 (C-5'), 117.1 (C-2'), 123.0 (C-1'), 123.1 (C-6'), 136.4 (C-3), 146.6 (C-3'), 145.0 (C-4'), 158.7 (C-9), 159.5 (C-2), 163.4 (C-5), 166.2 (C-7), 179.8 (C-4), 17.9 (C-6"), 72.1 (C-2"), 72.2 (C-4"), 72.3 (C-3"), 73.5 (C-5"), 103.7 (C-1") (Ishiguro et al. 1991).

Compound **9** yellow amorphous powder; ^{1}H NMR (500 MHz, MeOD) δ 0.92 (3H, d, *J* = 5.83. Hz, H-6"), 3.3 (1H, m, H-5"), 3.35 (1H, t, *J* = 1.0 Hz, H-4"), 3.70 (1H, dd, *J* = 3.5, 9.2 Hz, H-3"), 4.22 (1H, dd, *J* = 1.7, 3.3 Hz, H-2"), 5.37 (1H, d, *J* = 1.7 Hz, H-1"), 6.19 (1H, d, *J* = 2.1, Hz, H-6), 6.37 (1H, d, *J* = 2.1 Hz, H-8), 6.93 (2H, d, *J* = 8.8 Hz, H-3', H-5'), 7.76 (2H, d, *J* = 8.8 Hz, H-2', H-6'). ^{13}C NMR (125 MHz, MeOD) δ 95.2 (C-8), 100.4 (C-6), 105.9 (C-10), 116.8 (C-5′, C-3'), 122.9 (C-1'), 132.1 (C-2', C-6'), 136.4 (C-3), 158.7 (C-2), 159.5 (C-9), 161.9 (C-4'), 163.4 (C-5), 166.1 (C-7), 180.7 (C-4), 17.9 (C-6"), 71.6 (C-4"), 72.2 (C-2"), 72.3 (C-3"), 73.9 (C-5"), 103.7 (C-1") (Chen et al. 2004).

Compound **10** yellow amorphous powder; ^{1}H NMR (500 MHz, MeOD) δ 6.14 (1H, d, *J* = 2.0, Hz, H-6) 6.35 (1H, d, *J* = 1.9 Hz, H-8), 6.84 (1H, d, *J* = 8.5 Hz, H-3'), 7.59 (1H, dd, *J* = 2.1, 8.5 Hz, H-2'), 7.69 (1H, d, *J* = 2.0 Hz, H-6'). ^{13}C NMR (125 MHz, MeOD) δ 94.6 (C-8), 99.5 (C-6), 104.7 (C-10), 116.2 (C-2'), 116.4 (C-5'), 121.9 (C-6'), 124.4 (C-1'), 137.4 (C-3), 146.4 (C-3'), 148.2 (C-2), 149.0 (C-4'), 158.5 (C-9), 162.7 (C-5), 165.9 (C-7), 177.5 (C-4) (David et al. 1996).

Compound **11** off-white amorphous powder; ^{1}H NMR (300 MHz, MeOD) δ 4.45 (1H, d, *J* = 11.3 Hz, H-3), 4.82 (1H, d, *J* = 11.6 Hz, H-2), 5.88 (1H, d, *J* = 2.1 Hz, H-6), 5.92 (1H, d, *J* = 2.1 Hz, H-8), 6.53 (2H, s, H-2', H-6'). ^{13}C NMR (125 MHz, MeOD) δ 73.9 (C-3), 85.5 (C-2), 96.5 (C-8), 97.5 (C-6), 102.1 (C-10), 108.2 (C-2', C-6'), 129.3 (C-1'), 135.1 (C-4'), 147.1 (C-3', C-5'), 164.7 (C-9), 165.5 (C-5), 169.0 (C-7), 198.4 (C-4) (Sai et al. 2013).

Compound **12** white powder; HREIMS, *m/z* 345 $[M]^+$; HREIMS, *m/z* 345.1210 $[M+H]^+$ (calcd for $C_{15}H_{21}O_9$ 345.1210); ^{1}H NMR (500 MHz, DMSO–d_6) 2.56 (3H, s, O=C-C<u>H</u>$_3$), 3.21-3.31 (2H, m, H-4', H-5'), 3.39-3.46 (2H, m, H-2', H-3'), 3.68 (1H, dd, *J* = 5.4, 10.1 Hz, H-6'b), 3.86 (3H, s, -OCH_3), 4.09 (1H, dd, *J* = 5.2, 10.5 Hz, H-6'a), 5.12 (1H, d, *J* = 4.7 Hz, H-1'), 6.14 (1H, d, *J* = 2.3

Hz, H-5), 6.21 (1H, d, J = 2.3 Hz, H-3). ^{13}C NMR (125 MHz, DMSO–d_6) δ 33.3 (O=C-$\underline{C}H_3$), 56.5 (OCH_3), 61.1 (C-6'), 70.2 (C-4'), 73.5 (2'), 77.0 (3'), 77.7 (C-5'), 92.4 (C-5), 96.6 (C-3), 100.0 (C-1'), 106.8 (C-1), 163.1 (C-2), 164.2 (C-4), 165.8 (C-6), 203.5 (C=O) (Prasad 1999).

Evaluation of antioxidant activity by radical-based assays

Electron spin resonance spectroscopy (ESR)

DPPH and hydroxyl radicals were measured using a JEOL JES-TE300 ESR spectrometer operating with X-Band fashion at 100 kHz of modulation frequency and cylindrical cavity. The external calibration of the magnetic field was made with a Jeol ES-FC5 precision gauss meter and the frequency with a HP 5350B frequency counter. Using software ES-IPRITS-TE were made all spectral acquisitions, manipulations and simulations. All compounds (**1**-**12**) were prepared at stock concentration and prepared to corresponding concentrations (0, 15.0, 30.0, 60.0 and 12.0 μM) using DMSO and measured using quartz flat tube.

DPPH radical scavenging assay by ESR

DPPH radical scavenging activity was described by the next method (Kim et al. 2018). To 10 μL of inhibitors or trolox as control were added 170 μL of 0.15 mM DPPH which was prepared in ethanol. Measurement conditions: magnetic field, 339.5 mT; microwave frequency, 9.42 GHz; power, 5 mW; sweep time, 2 min; modulation, 100 kHz; amplitude, 1 × 100; time constant 0.1 sec. Inhibitors DPPH radical scavenging rates were calculated using the next equation:

$$\text{Radical scavenging activity (\%)} = [(I_0\text{-}I)/I_0] \times 100 \quad (1)$$

where I_0 and I are the ESR intensity in the absence and presence of compound, respectively.

Hydroxyl radical scavenging assay by ESR

Hydroxyl radical scavenging activity was described by the next method (Kim et al. 2018). Hydroxyl radical scavenging activity was determined on the base of Fenton reaction generated radical. To 20 μL of inhibitors or control (trolox) added 50 μL of 0.3 M DMPO in 10 mM phosphate buffer (pH 7.4), 50 μL of 30 % H_2O_2 and 30 μl of 10 mM fresh $FeSO_4$. Measurement conditions were the same to DPPH RSA described just before, with only one change in power to 1 mW. The hydroxyl radical scavenging rate of inhibitors were calculated using equation (1).

Oxygen radical absorbance capacity (ORAC)

The ORAC assay based in inhibition of the peroxyradical-induced oxidation initiated by thermal decomposition of azocompounds such as [2,2'-azobis(amino-propane) dihydrochlorine(AAPH)] (Kim et al. 2018). AAPH (80 mg) was made to the final concentration of 29.5 mM. A fluorescein stock solution (4μM) was made in 75 mM phosphate buffer (pH 7.4), prior to use, was diluted 1:200 with phosphate buffer (pH 7.4). Briefly, to 150 μL of sodium fluorescein working solution was added, and blank with 25 μL of 75 mM phosphate buffer (pH 7.4), inhibitors as 25 μL of Trolox or compounds, and

incubated for a 30 min. at 37 °C. Addition of 25 µL of AAPH started the reaction. Fluorescence measured at the excitation of 480 nm and emission 520 nm wavelength. ORAC values were determined on Trolox standard curve by the graph of Net AUC on the y-axis against as equivalent Trolox concentration on the x-axis:

$$AUC = 1 + RFU_1/RFU_0 + RFU_2/RFU_0 + RFU_3/RFU_0 + \ldots + RFU_{59}/RFU_0 + RFU_{60}/RFU_0 \quad (2)$$

$$\text{Net AUC} = \text{AUC (Antioxidant)} - \text{AUC (blank)} \quad (3)$$

LC-ESI MS/MS analysis

The relative abundance of the isolated compounds (**1-12**) in the crude extract was analysed by HPLC (SCIEX QTRAP 3200), equipped with an electrospray ionization source (ESI) and triple quadrupole-ion trap mass analyser. ESI was worked in the positive-ion mode, with following conditions: capillary temperature 500 °C, curtain gas at 20 psi, nebulizer gas at 50 psi, and positive ionization mode source voltage – 4500V. The chromatographic columns were using a Zorbax Bonus RP column (4.6 x 150mm, 5µM, Agilent, USA). Absorbance was measured at 280 nm. A linear gradient profile of mobile phase, comprising water/0.1% acetic acid (solvent A) and acetonitrile (solvent B), 15% B (0-1 min), 30% B (1-3 min), 40% B (3-4 min), 50% B (4-13 min), 100% B (13-25 min) was applied at flow rate 0.5mL/min. the column was kept at room temperature and 10 µL of sample were injected into the HPLC system.

DNA oxidation

Hydroxyl radical induced DNA damaged assay was determined according to the next method (Kim et al. 2018). 1 µL of pBR322 plasmid DNA (0.35 µg/mL) in 9 µL of phosphate buffer (pH 7.4), 2 µL of 1mM $FeSO_4$, 5 µL of inhibitors (**1-9**) or Trolox as control and 3 µL of 30 % H_2O_2 were mixed in eppendorf tube, incubated at 37 °C for 36 min in the dark condition. After, 5 µL of a mixture and 1 µL of 6× DNA loading buffer (Enzynomics, Korea) were mixed and loaded onto a 0.8% agarose gel containing 1× RedSafe, DNA staining solution (Intron biotechnology, Korea) in TAE buffer (40 mM Tris-acetate and 1 mM EDTA). Then gel electrophoresed for 30 min at 85 V. Finally, the DNA in the gel were recorded in Image Lab Software. Inhibition of DNA damage (%) and protective effect were calculated using the equation (4) and (5), respectively:

$$\text{DNA damage (\%)} = \text{ocDNAband intensity/pBR322 DNA band intensity} \times 100 \quad (4)$$

$$\text{DNA retention (\%)} = \text{intensity of scDNA with the oxidative radical and compounds/ intensity of scDNA in control} \times 100 \quad (5)$$

Statistical analysis

All experiments were carried out at least in triplicates. The results were analysed to variance analysis using Sigma Plot (version 10.0, Systat Software, Inc., San Jose, CA). Differences were considered significant at $p < 0.05$.

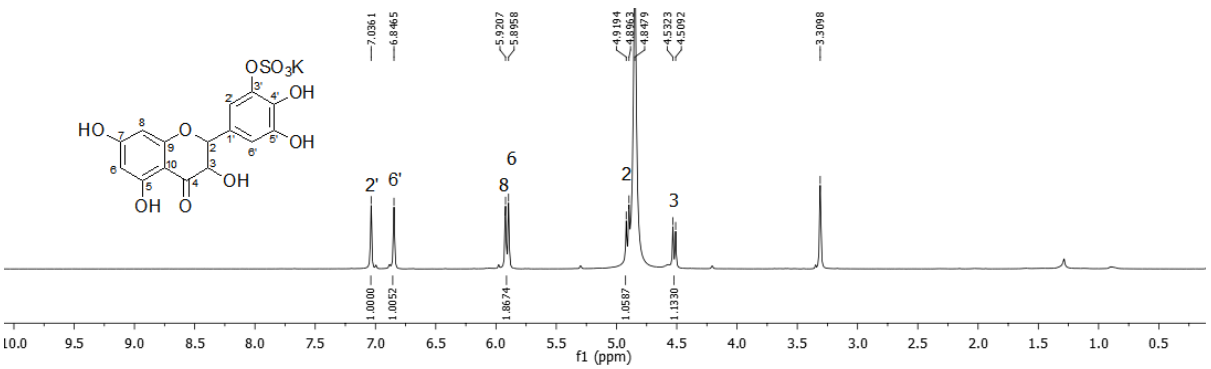

Figure S1. ^{1}H NMR spectrum of compound **1** (500 MHz, MeOD)

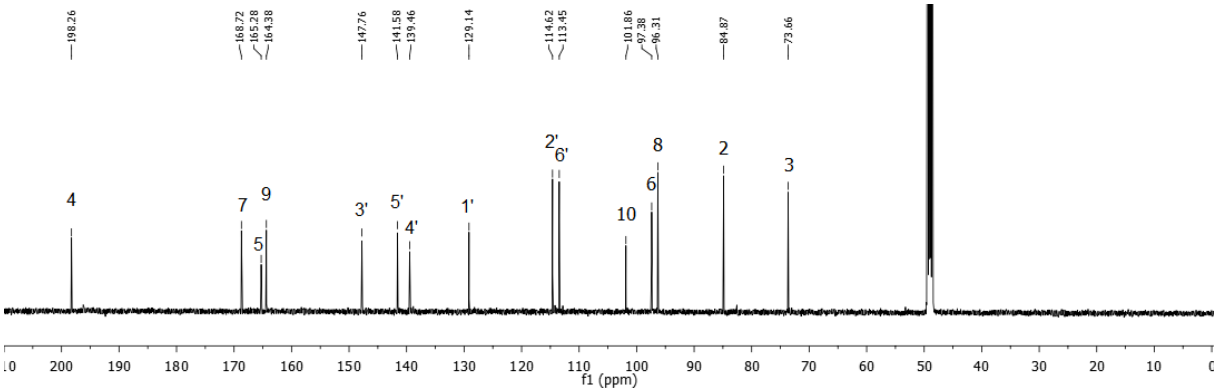

Figure S2. ^{13}C NMR spectrum of compound **1** (125 MHz, MeOD)

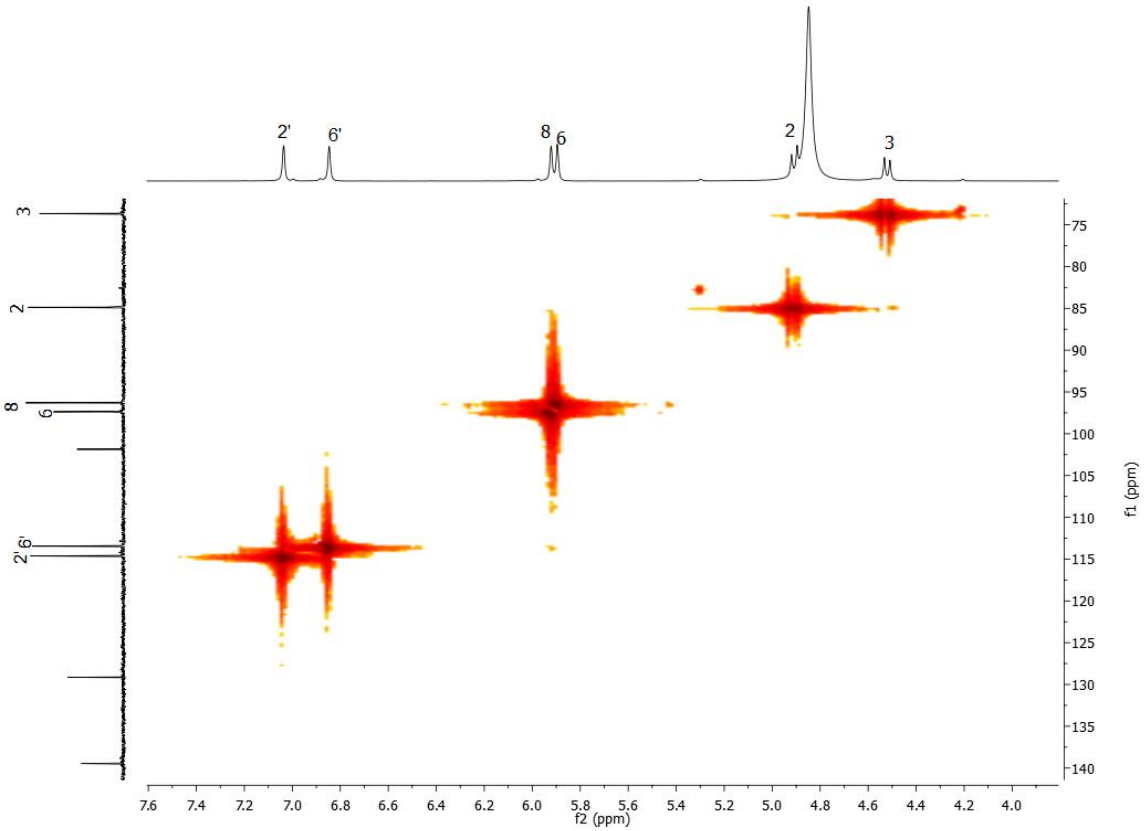

Figure S3. HMQC NMR spectrum of compound **1**.

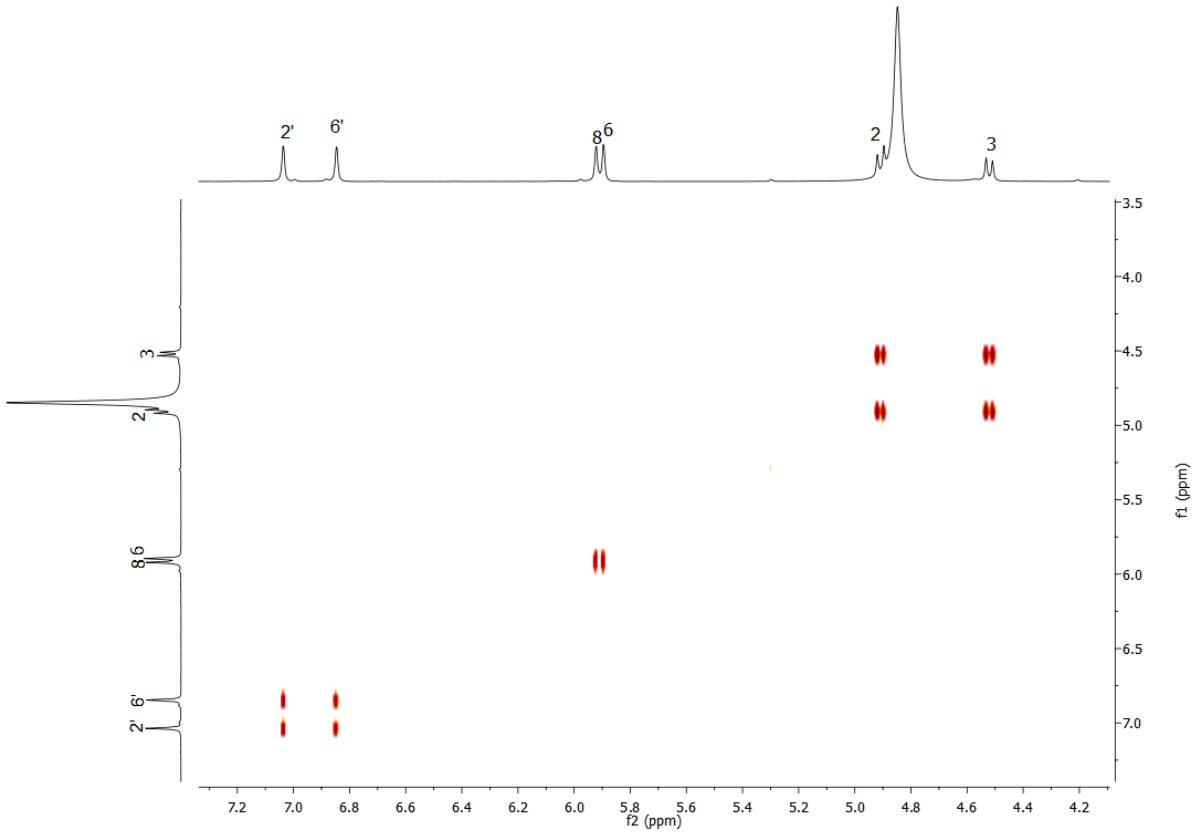

Figure S4. COSY NMR spectrum of compound **1**.

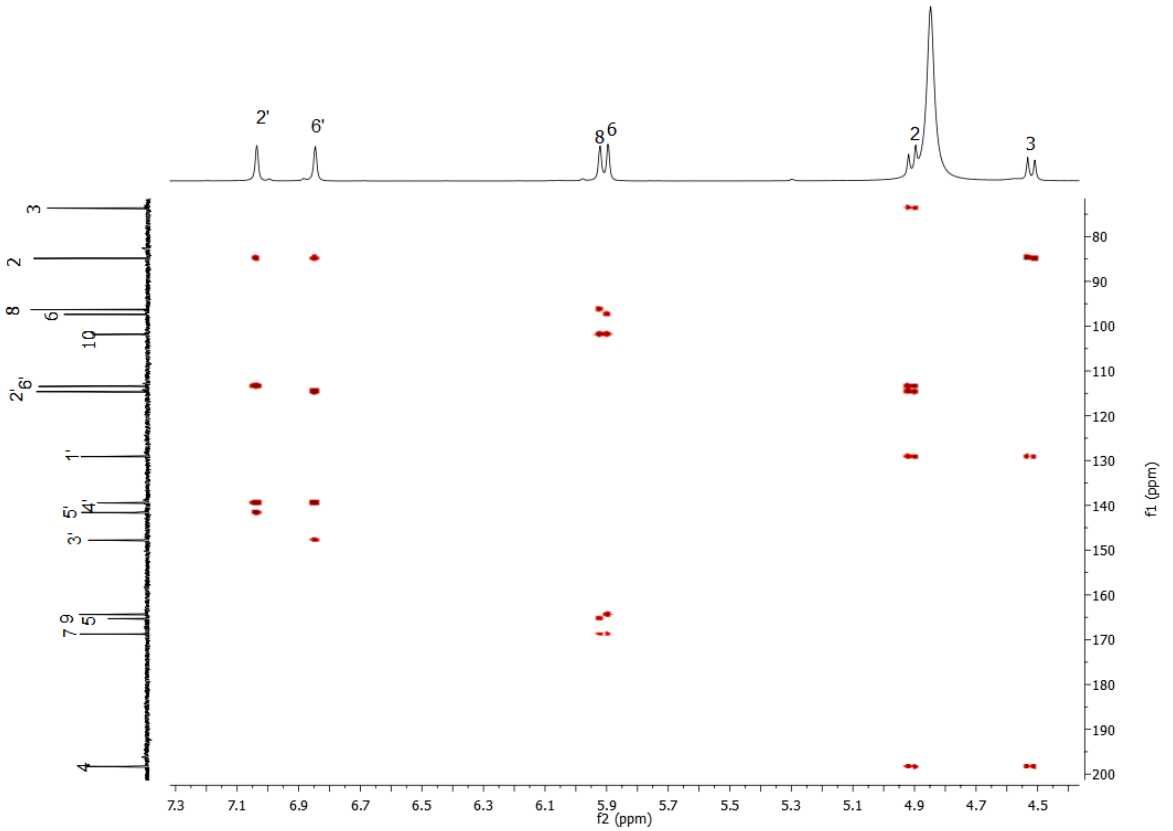

Figure S5. HMBC NMR spectrum of compound **1**.

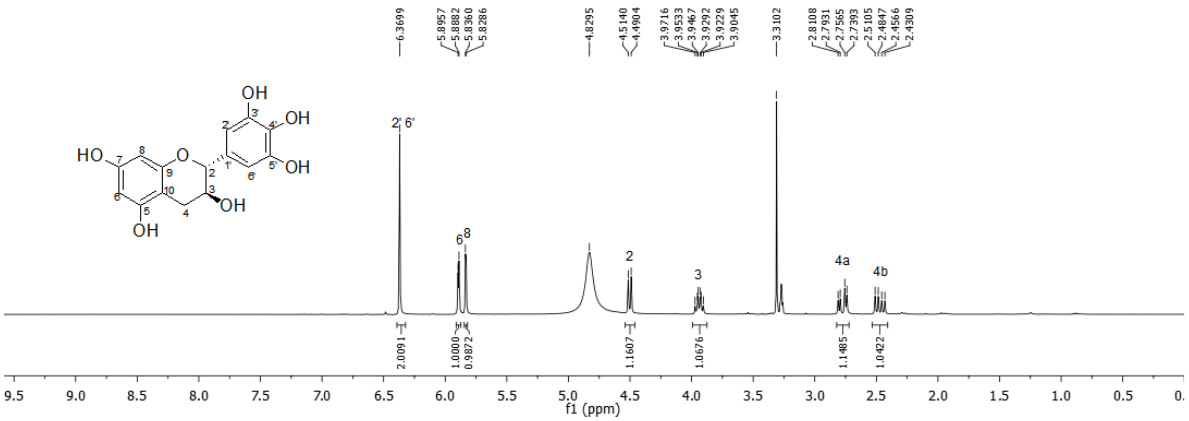

Figure S6. ^{1}H NMR spectrum of compound **2** (300 MHz, MeOD)

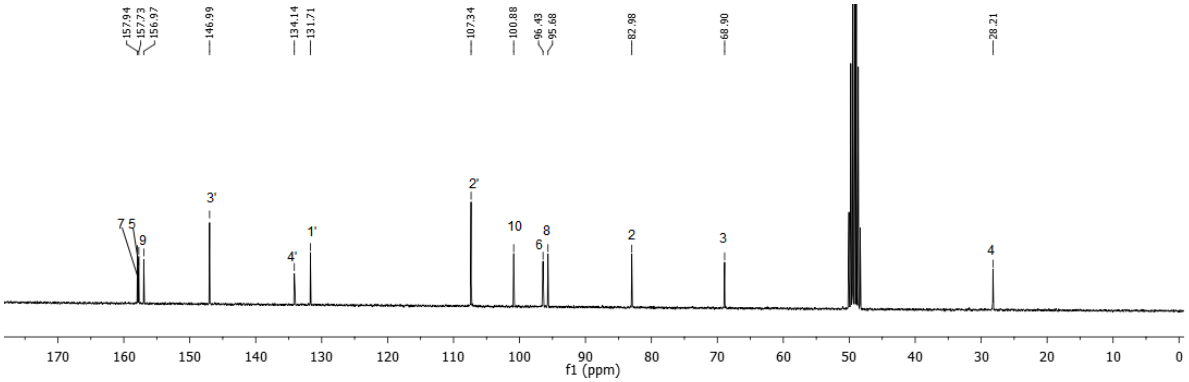

Figure S7. ^{13}C NMR spectrum of compound **2** (125 MHz, MeOD)

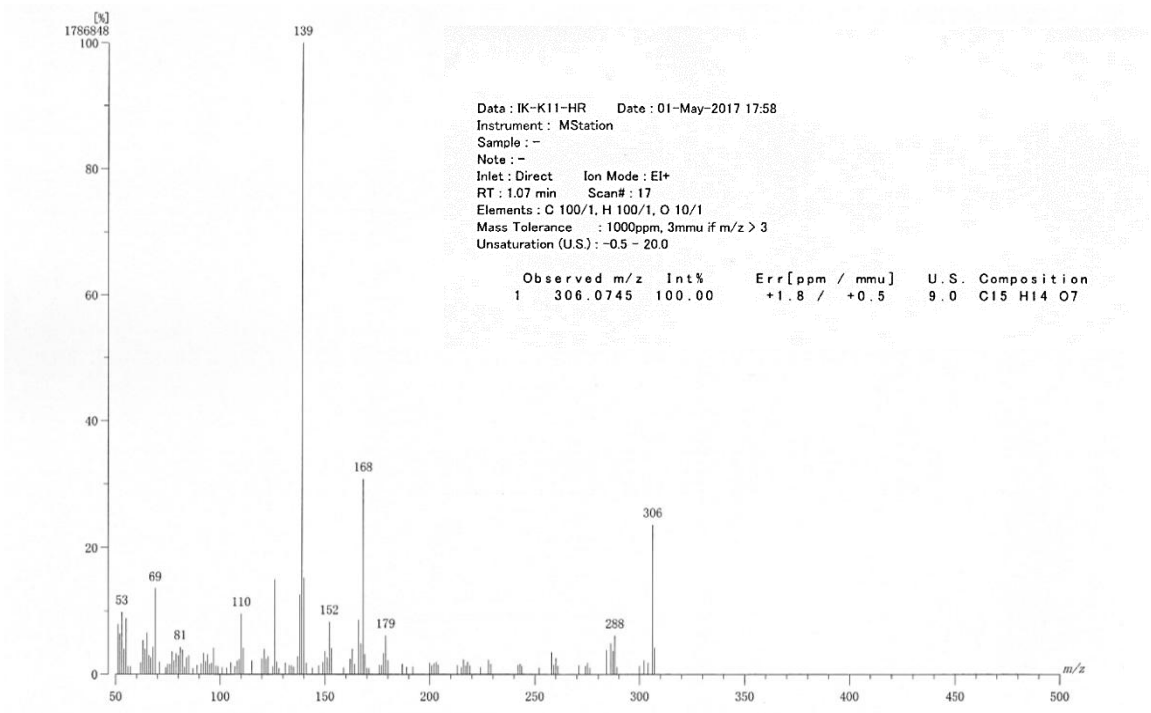

Figure S8. EIMS spectra and HREIMS data of compound **2.**

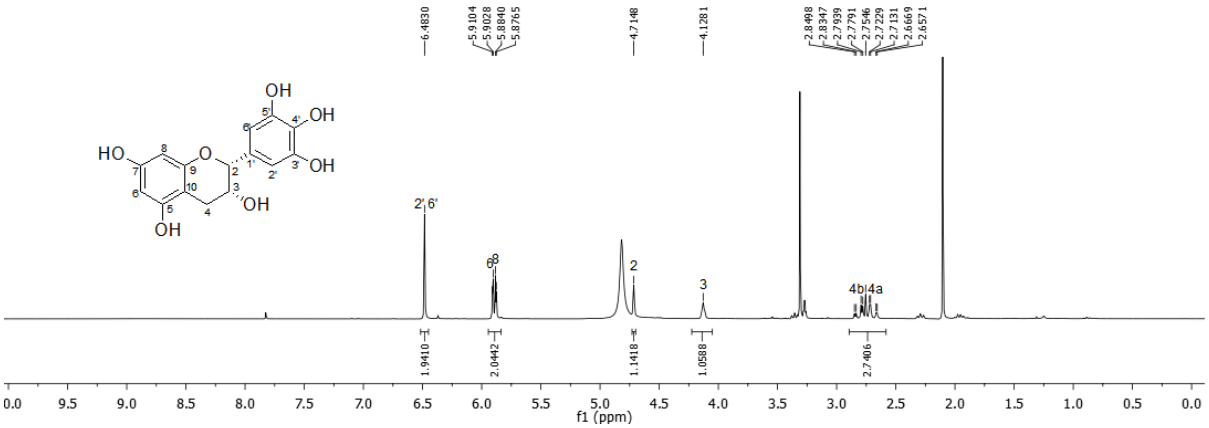

Figure S9. ^{1}H NMR spectrum of compound **3** (300 MHz, MeOD)

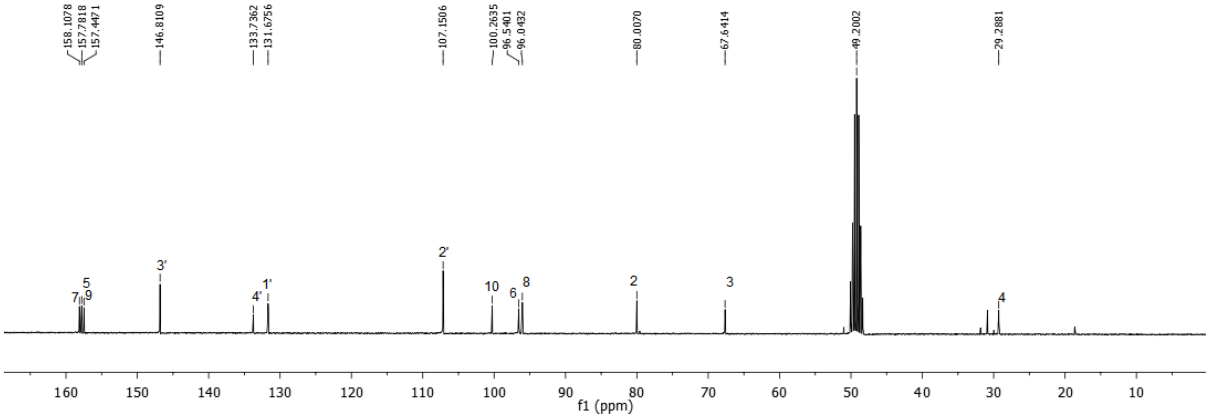

Figure S10. ^{13}C NMR spectrum of compound **3** (125 MHz, MeOD)

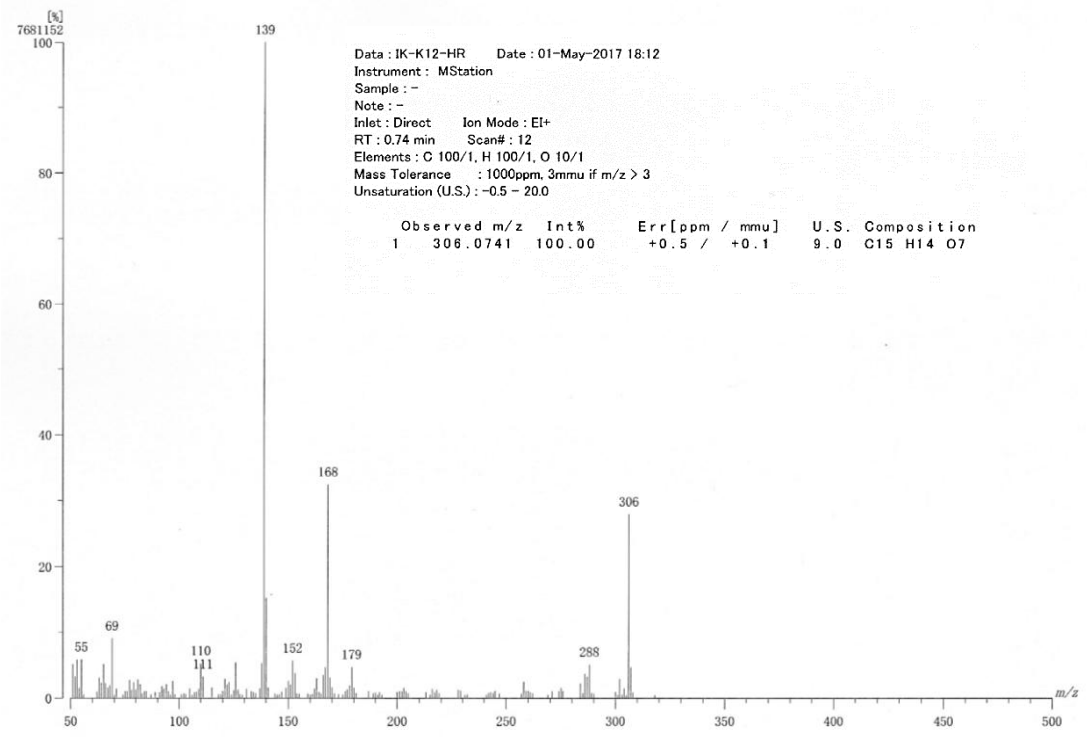

Figure S11. EIMS spectra and HREIMS data of compound **3.**

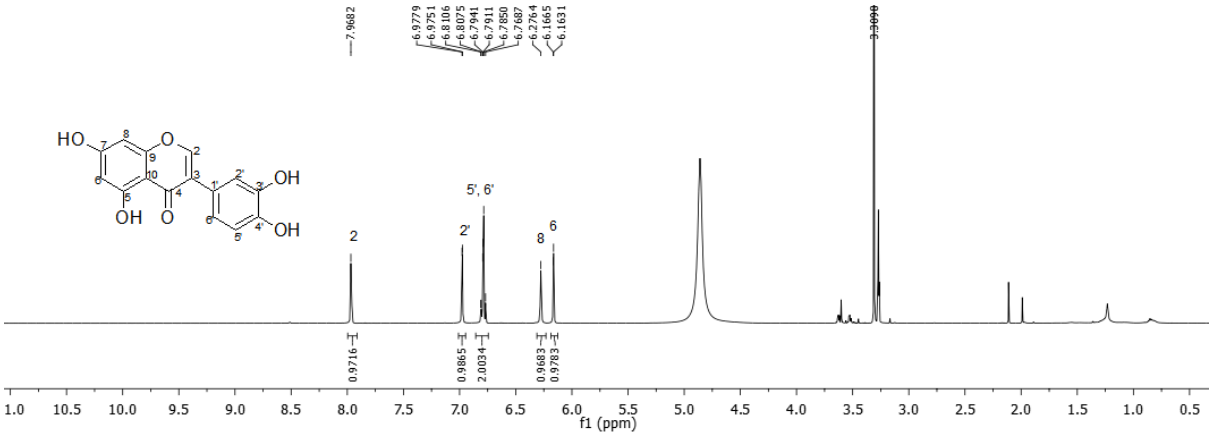

Figure S12. ^{1}H NMR spectrum of compound **4** (500 MHz, MeOD)

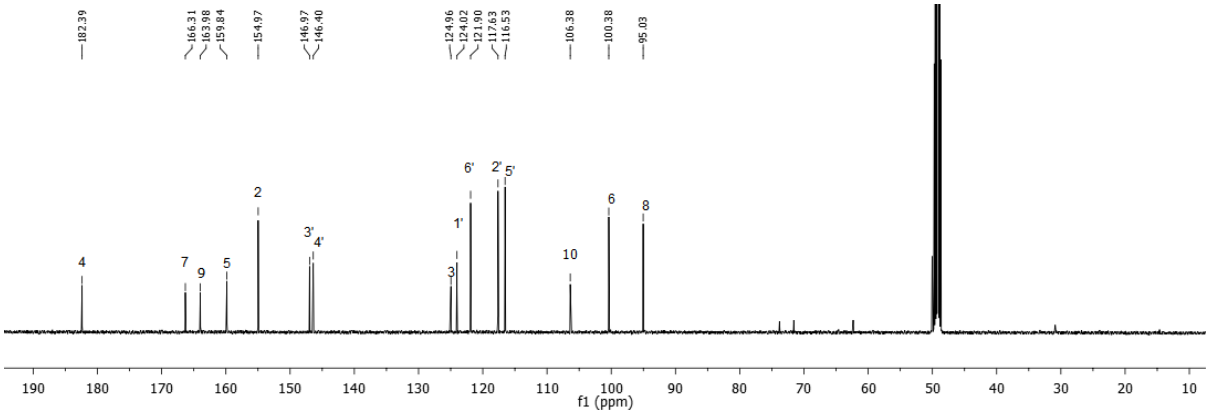

Figure S13. ^{13}C NMR spectrum of compound **4** (125 MHz, MeOD)

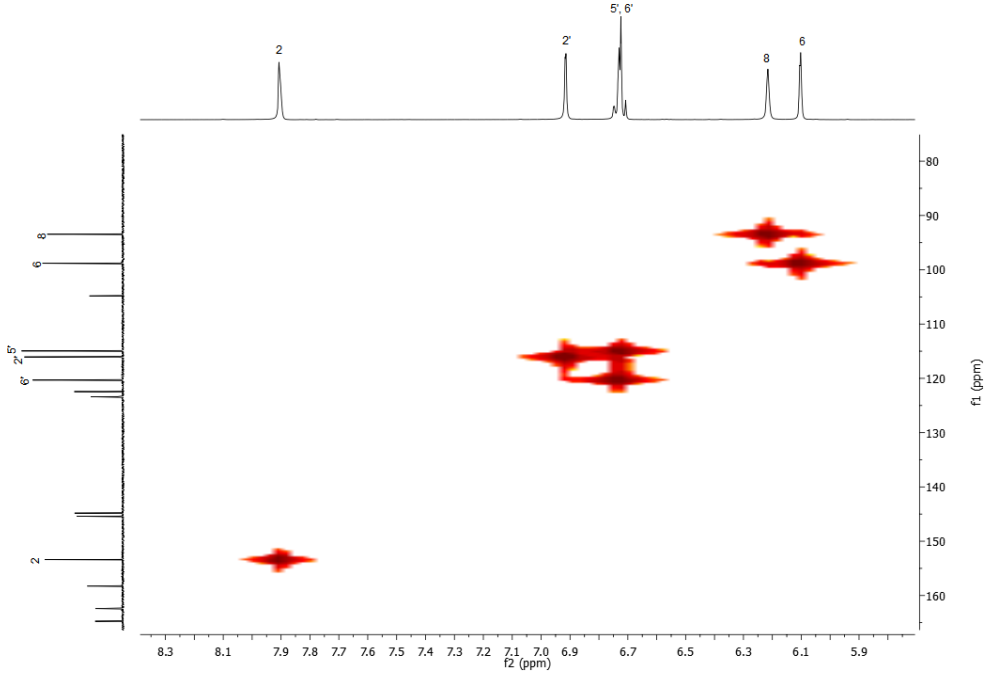

Figure S14. HMQC spectrum of compound **4**.

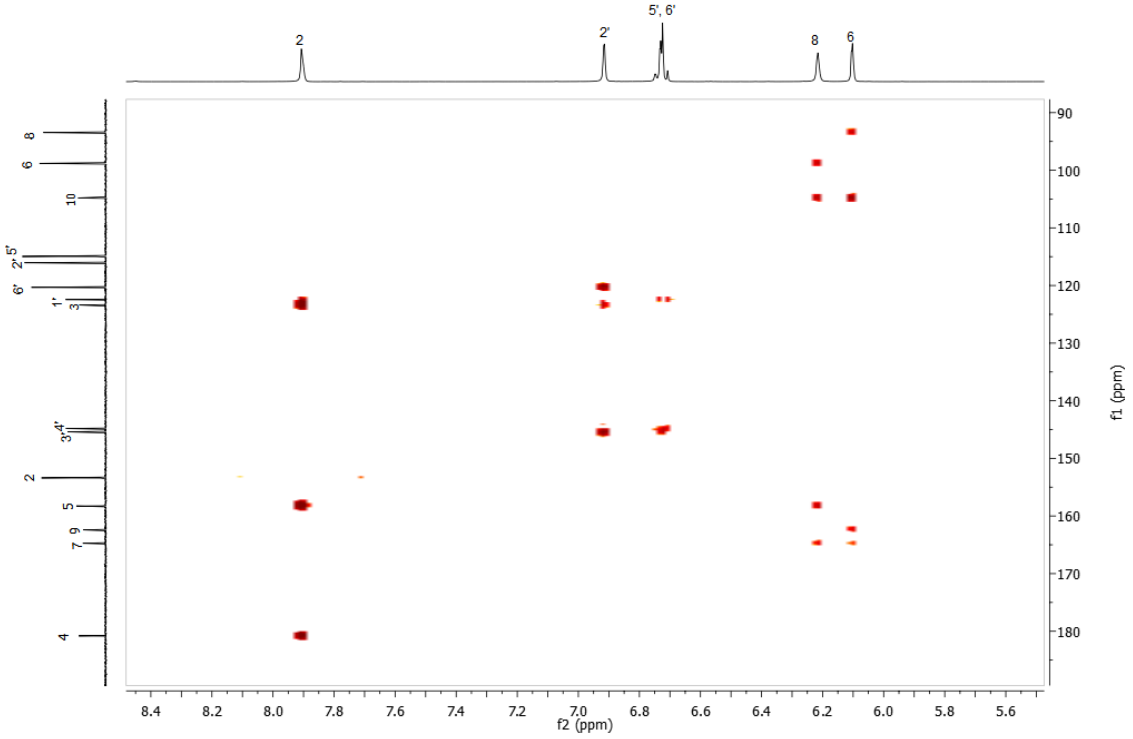

Figure S15. HMBC spectrum of compound **4**.

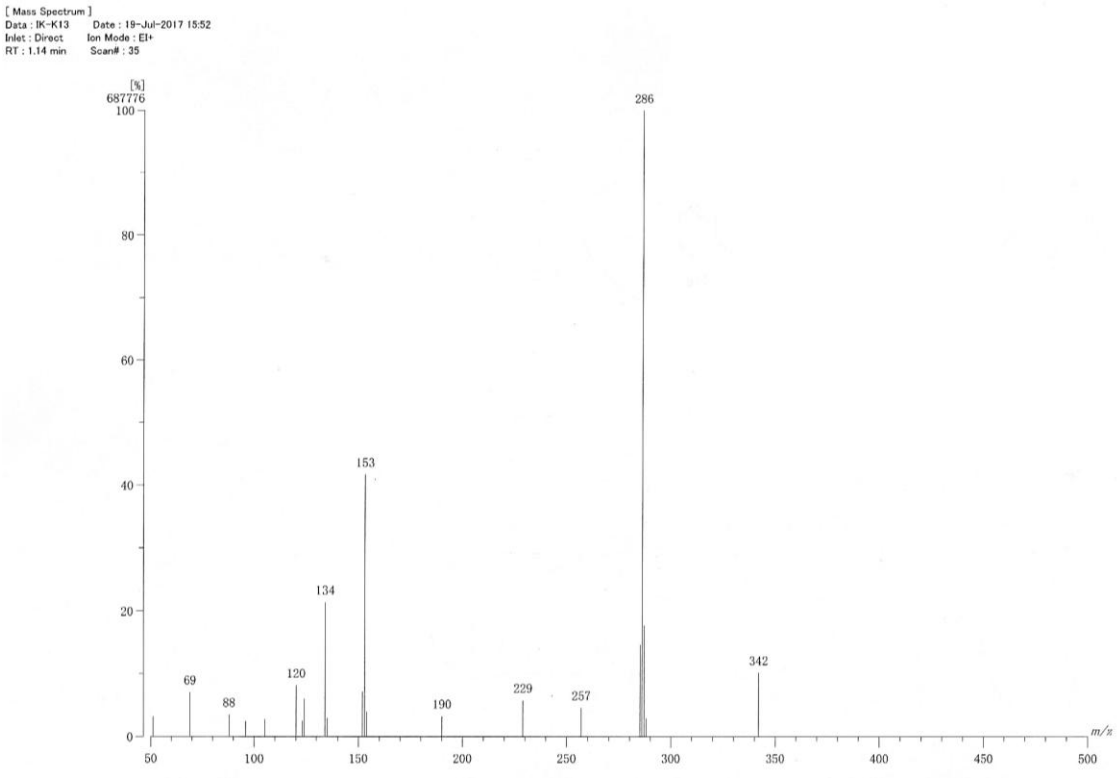

Figure S16. EIMS spectra of compound **4.**

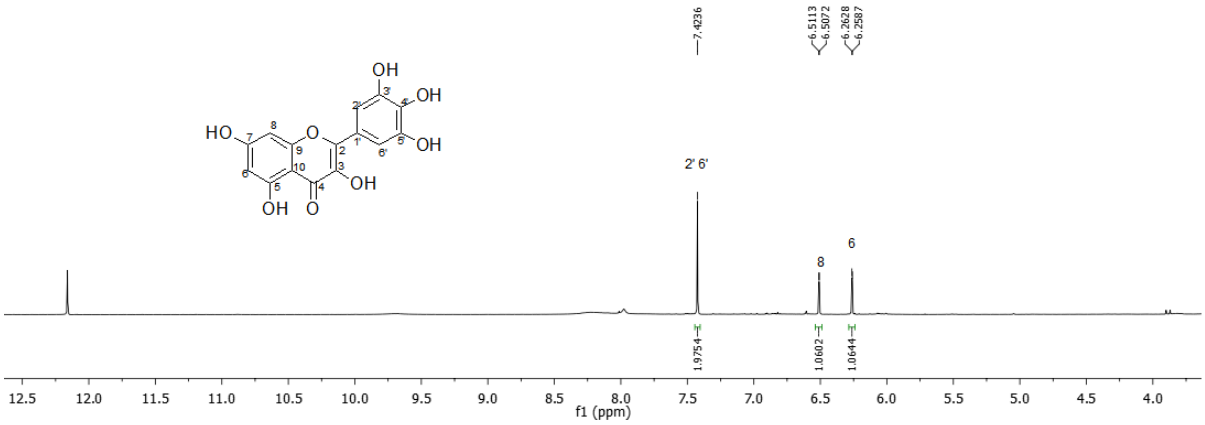

Figure S17. ^{1}H NMR spectrum of compound **5** (500 MHz, $(CD_3)_2CO$)

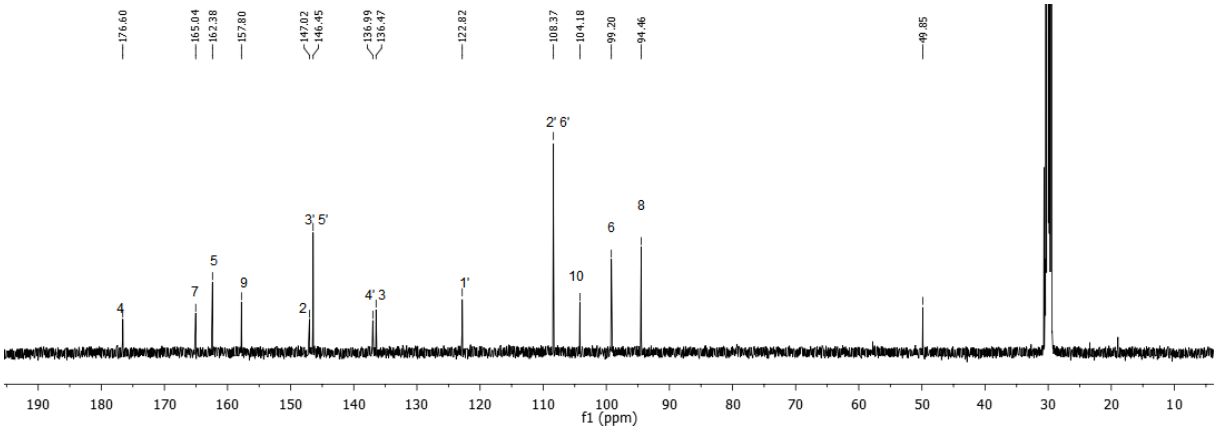

Figure S18. ^{13}C NMR spectrum of compound **5** (125 MHz, $(CD_3)_2CO$)

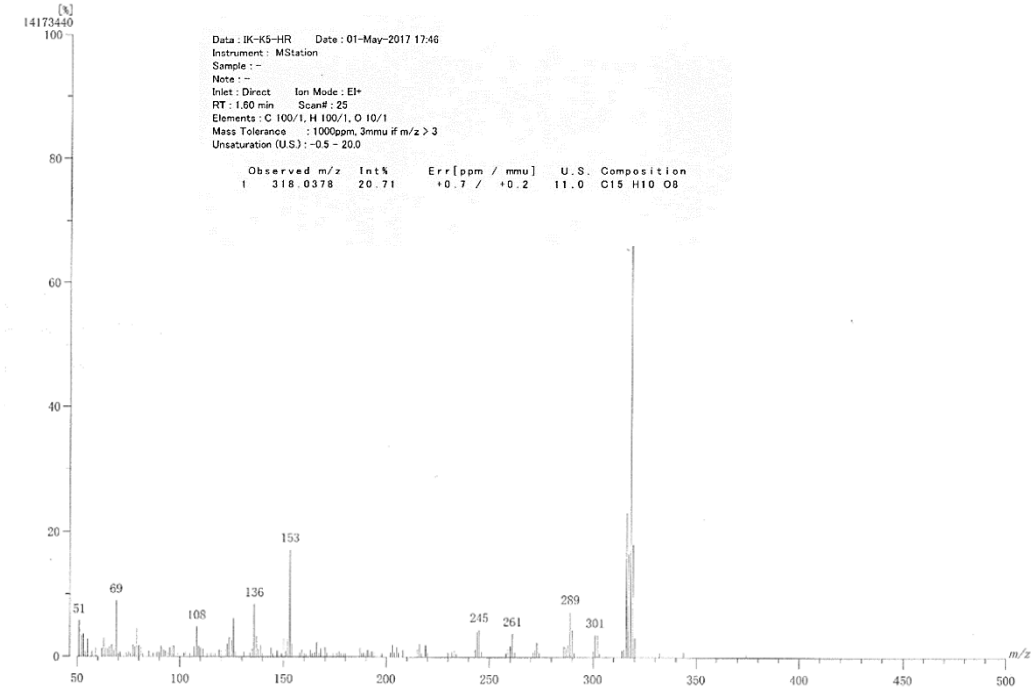

Figure S19. EIMS spectra and HREIMS data of compound **5.**

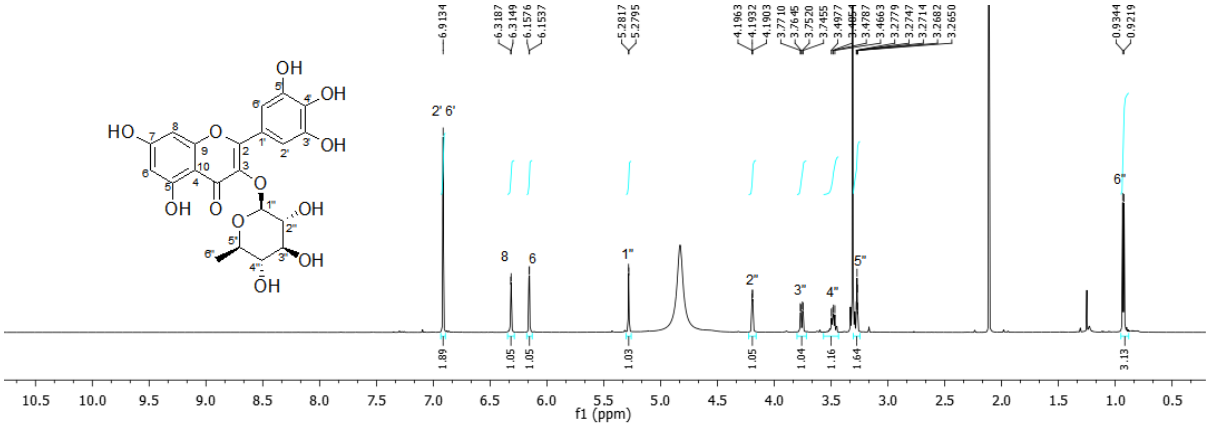

Figure S20. ^{1}H NMR spectrum of compound **6** (500 MHz, MeOD)

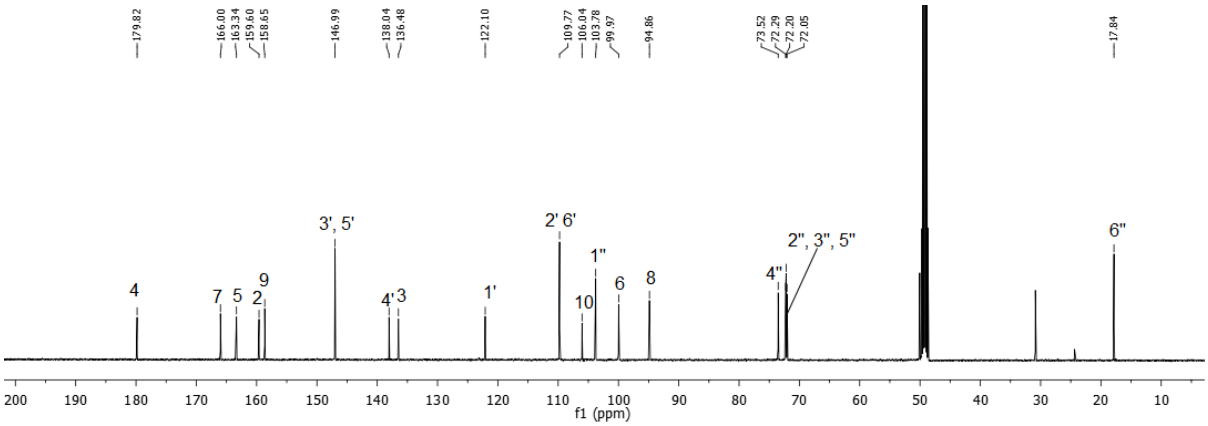

Figure S21. ^{13}C NMR spectrum of compound **6** (125 MHz, MeOD)

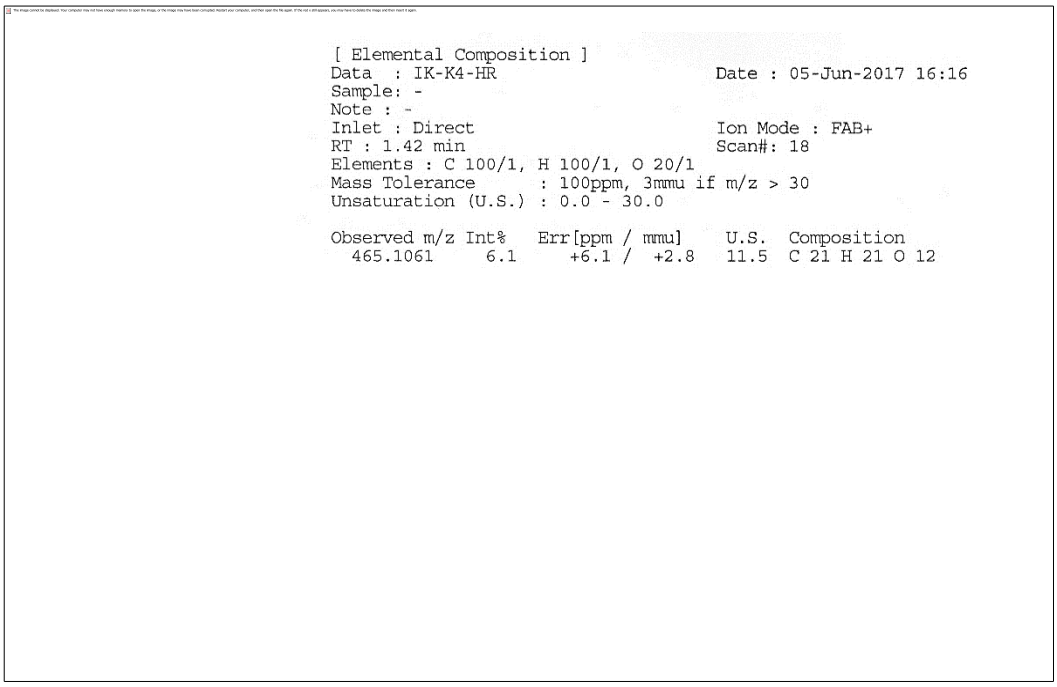

```
[ Elemental Composition ]
Data  : IK-K4-HR                        Date : 05-Jun-2017 16:16
Sample: -
Note : -
Inlet : Direct                          Ion Mode : FAB+
RT : 1.42 min                           Scan#: 18
Elements : C 100/1, H 100/1, O 20/1
Mass Tolerance          : 100ppm, 3mmu if m/z > 30
Unsaturation (U.S.) : 0.0 - 30.0

Observed m/z Int%   Err[ppm / mmu]    U.S.  Composition
  465.1061     6.1     +6.1 /  +2.8   11.5  C 21 H 21 O 12
```

Figure S22. FABMS spectra and HRFABMS data of compound **6.**

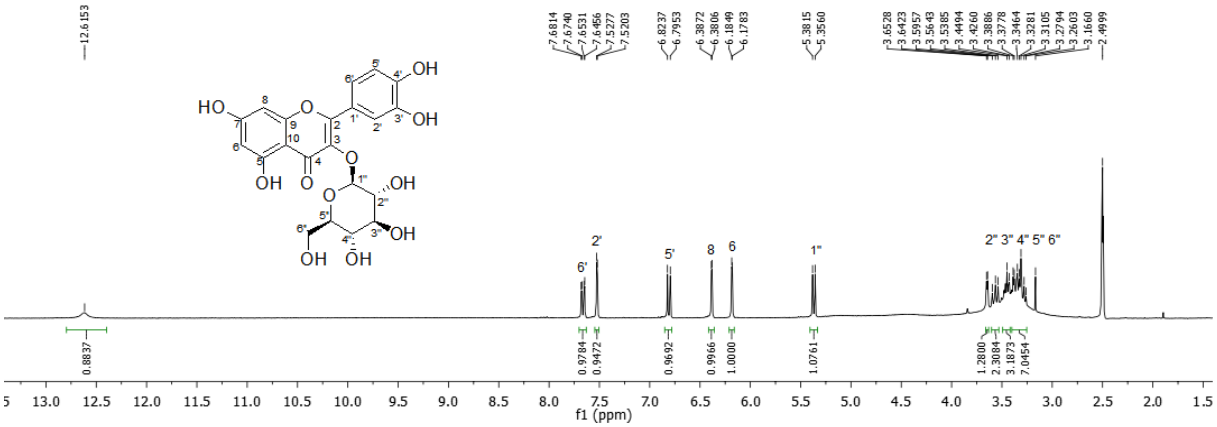

Figure S23. ^{1}H NMR spectrum of compound **7** (300 MHz, DMSO-d_6)

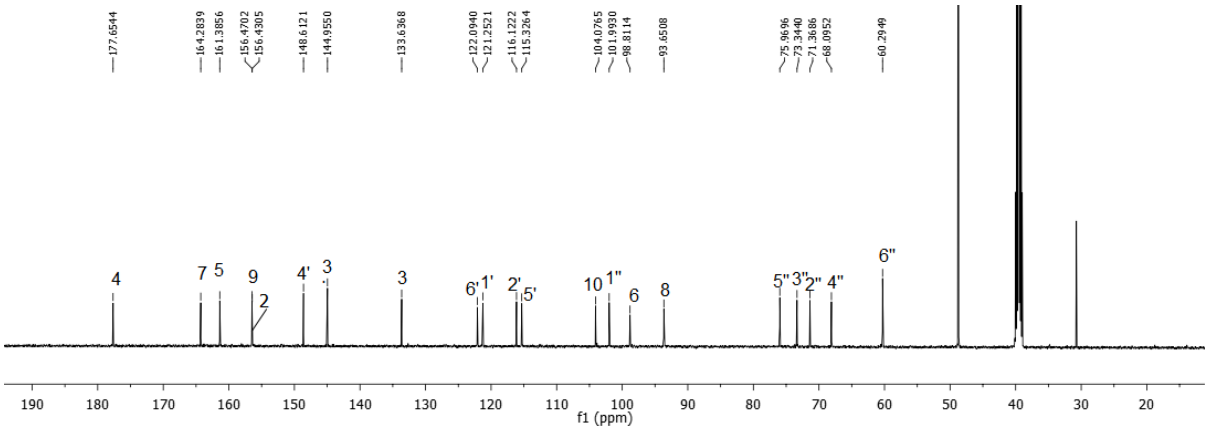

Figure S24. ^{13}C NMR spectrum of compound **7** (125 MHz, DMSO-d_6)

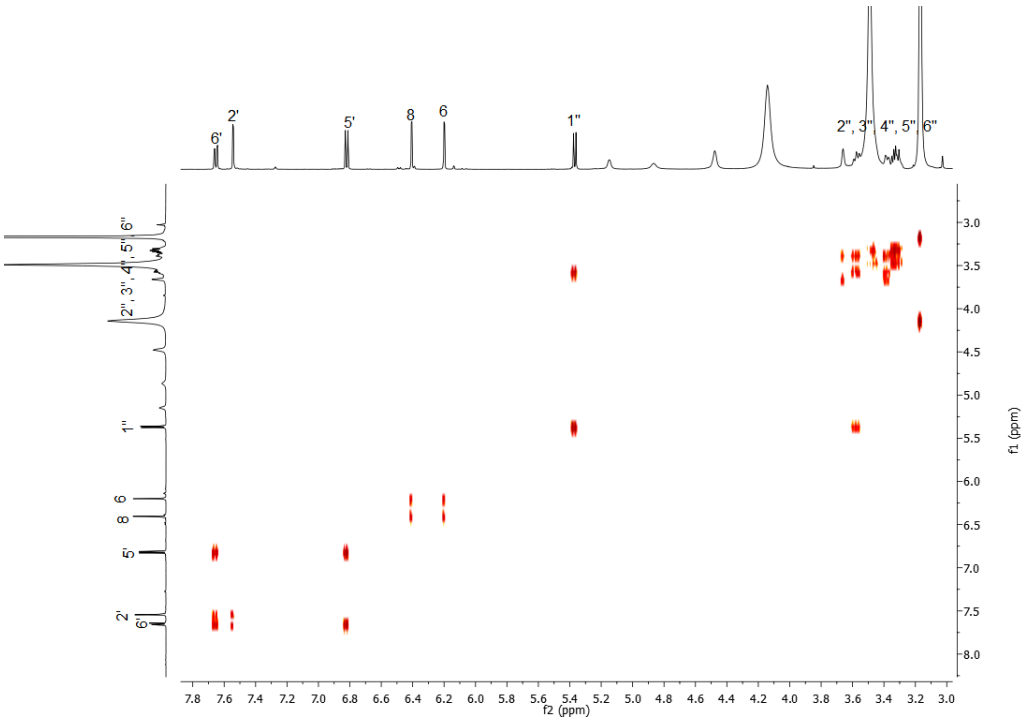

Figure S25. COSY spectrum of compound **7**.

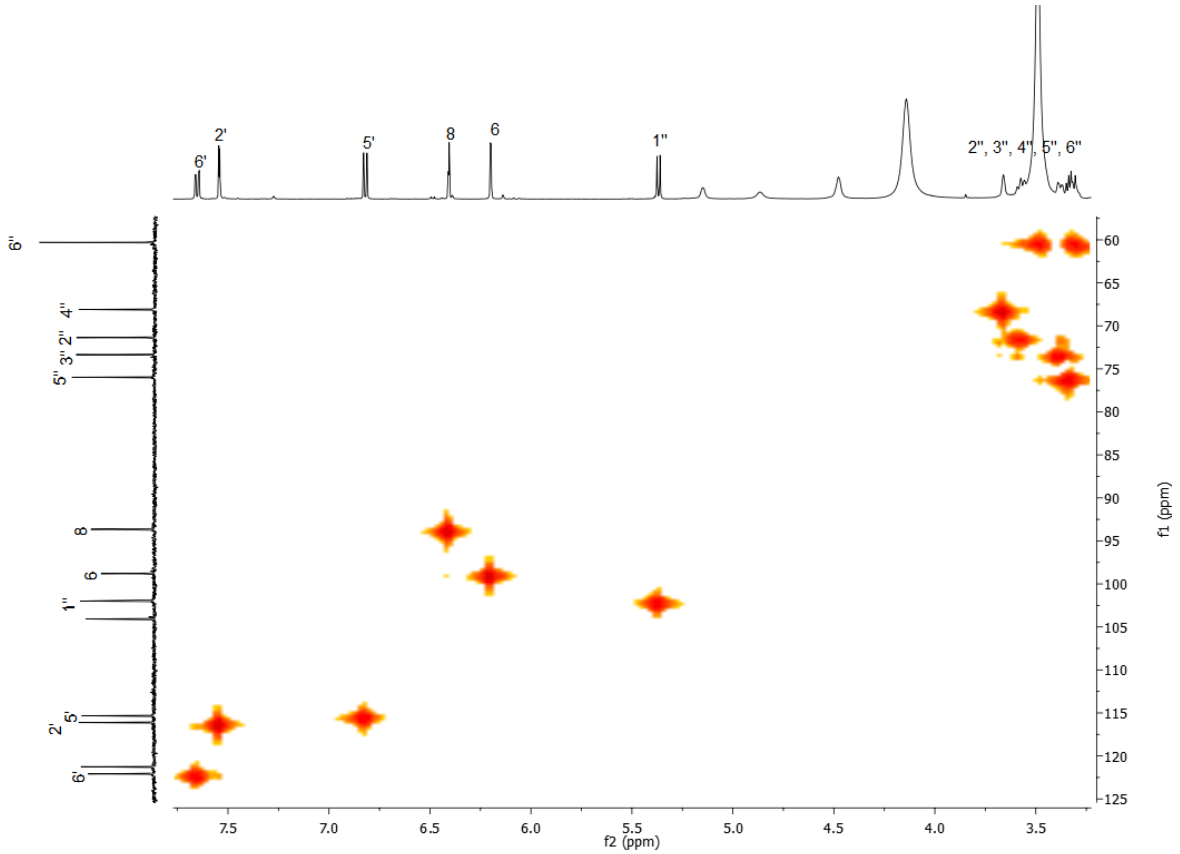

Figure S26. HMQC spectrum of compound **7**.

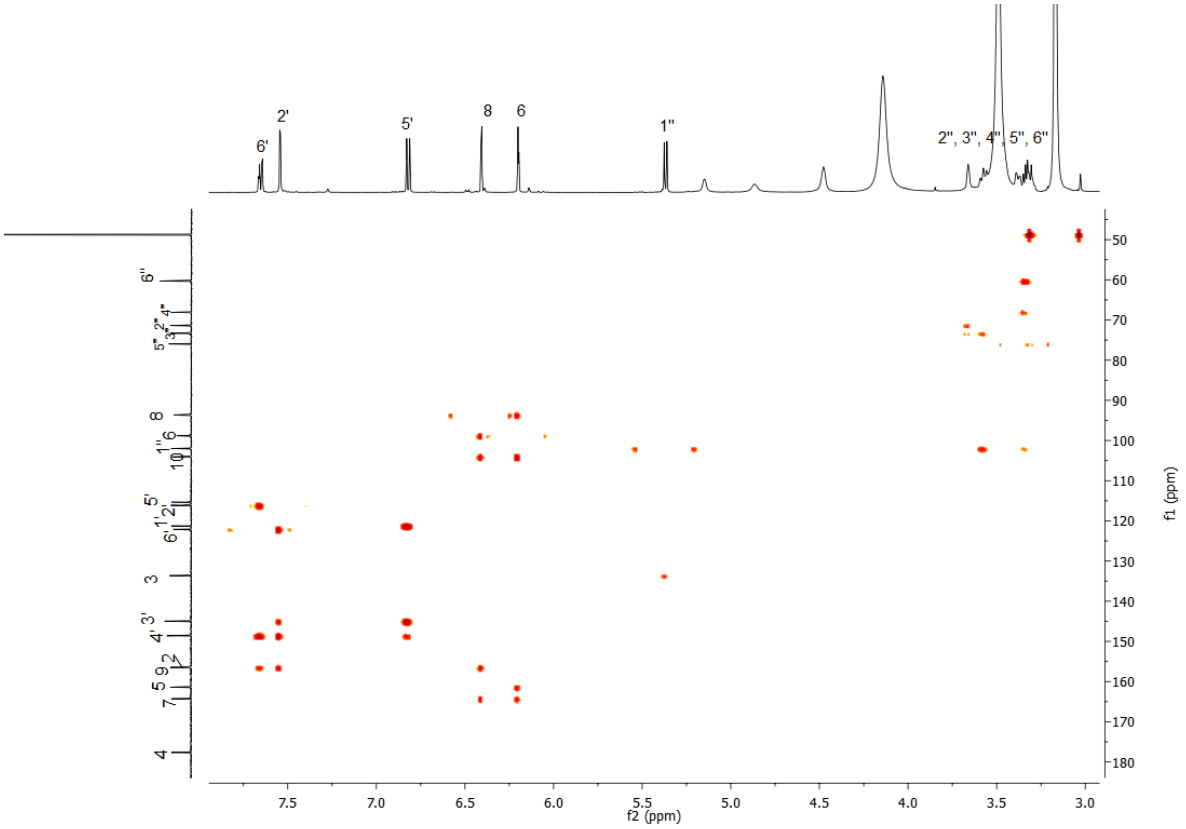

Figure S27. HMBC spectrum of compound **7**.

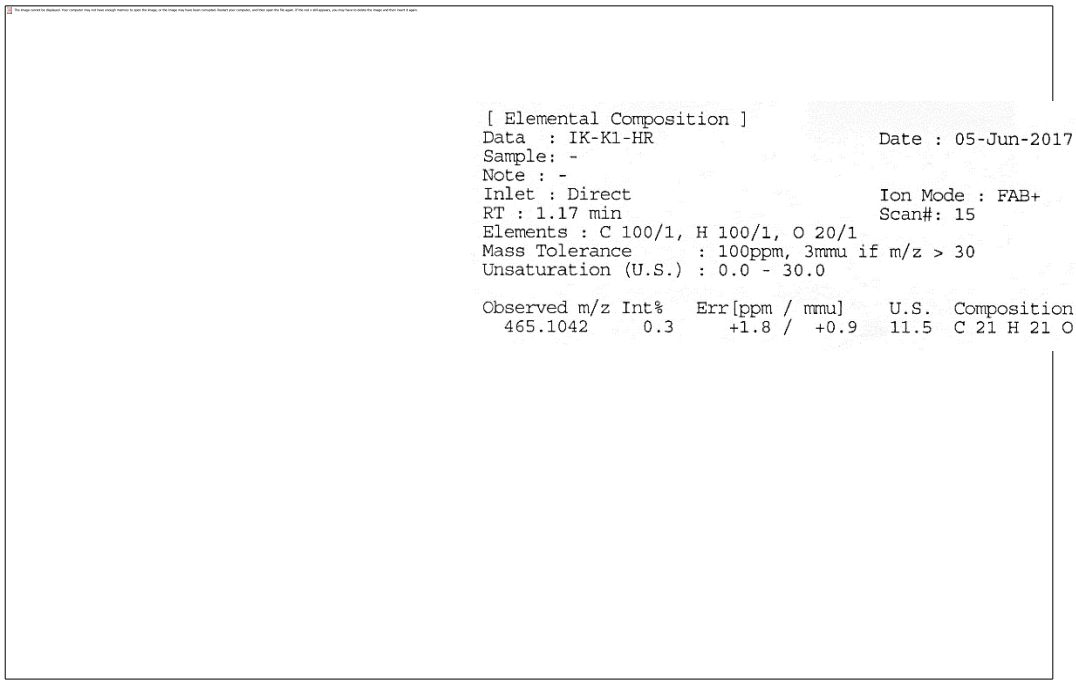

```
[ Elemental Composition ]
Data  : IK-K1-HR                          Date : 05-Jun-2017 16:11
Sample: -
Note : -
Inlet : Direct                            Ion Mode : FAB+
RT : 1.17 min                             Scan#: 15
Elements : C 100/1, H 100/1, O 20/1
Mass Tolerance      : 100ppm, 3mmu if m/z > 30
Unsaturation (U.S.) : 0.0 - 30.0

Observed m/z Int%   Err[ppm / mmu]    U.S.  Composition
  465.1042     0.3     +1.8 /  +0.9   11.5  C 21 H 21 O 12
```

Figure S28. FABMS spectra and HRFABMS data of compound **7.**

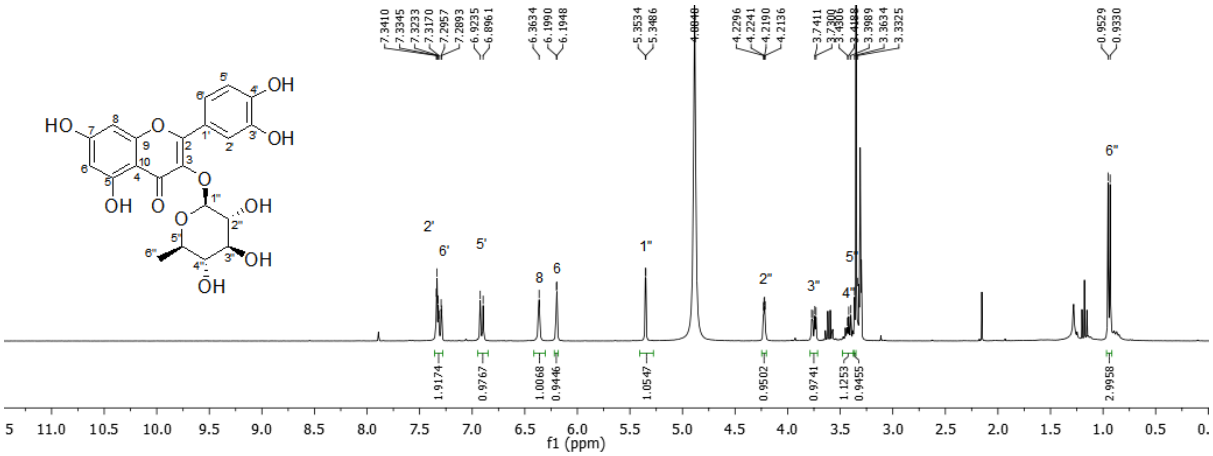

Figure S29. ^{1}H NMR spectrum of compound **8** (300 MHz, MeOD)

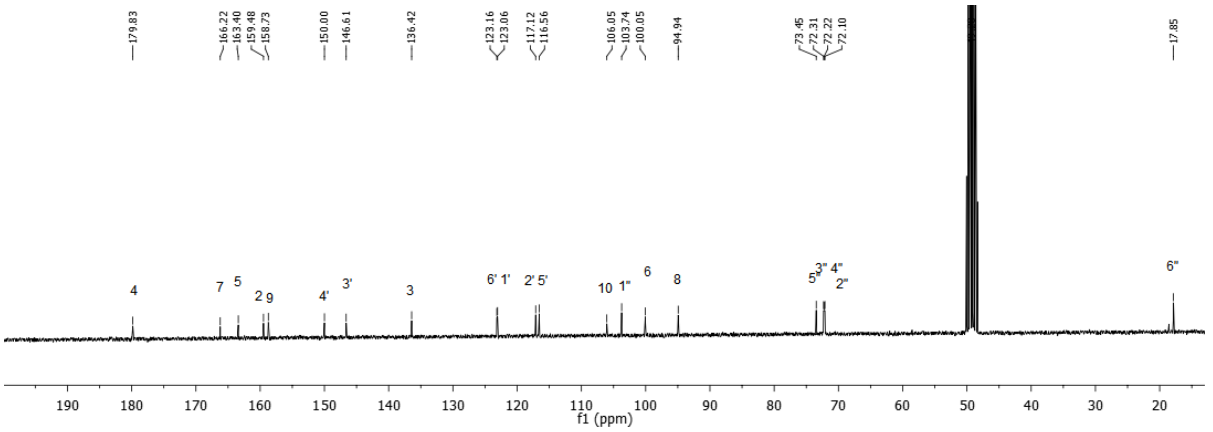

Figure S30. ^{13}C NMR spectrum of compound **8** (125 MHz, MeOD)

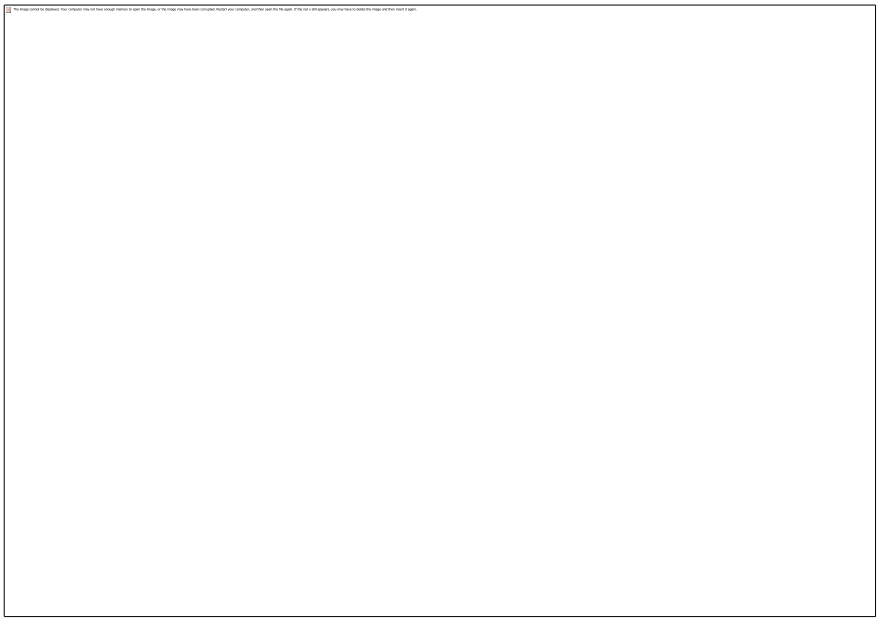

Figure S31. FABMS spectra of compound **8.**

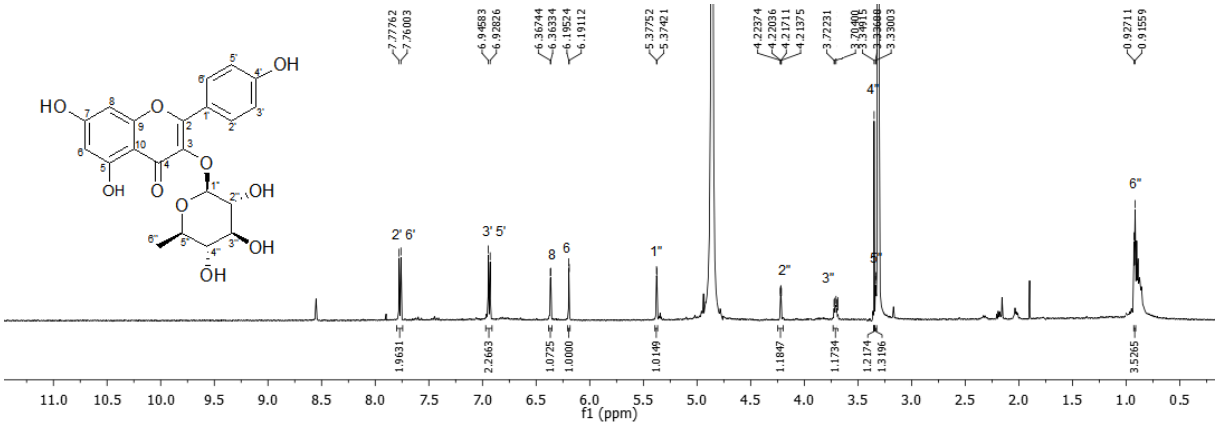

Figure S32. ^{1}H NMR spectrum of compound **9** (500 MHz, MeOD)

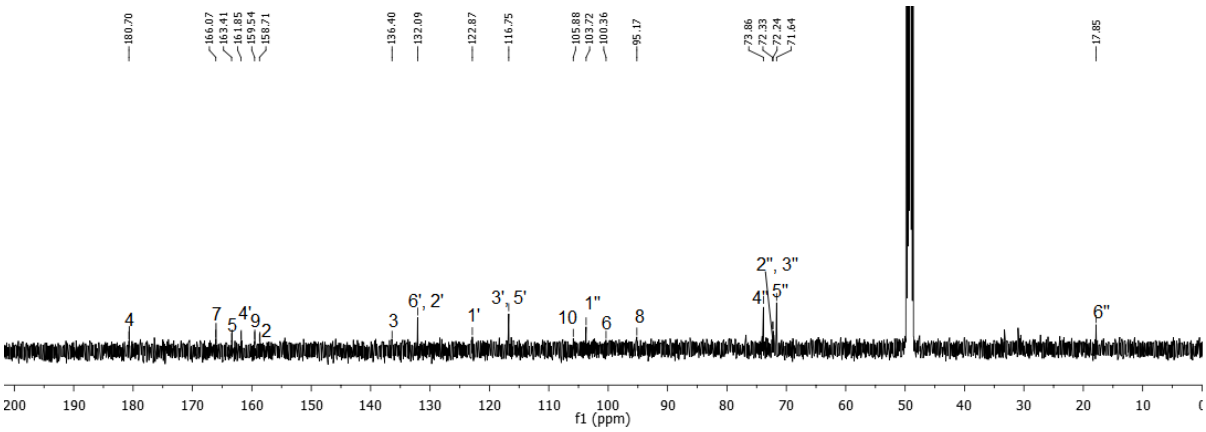

Figure S33. ^{13}C NMR spectrum of compound **9** (125 MHz, MeOD)

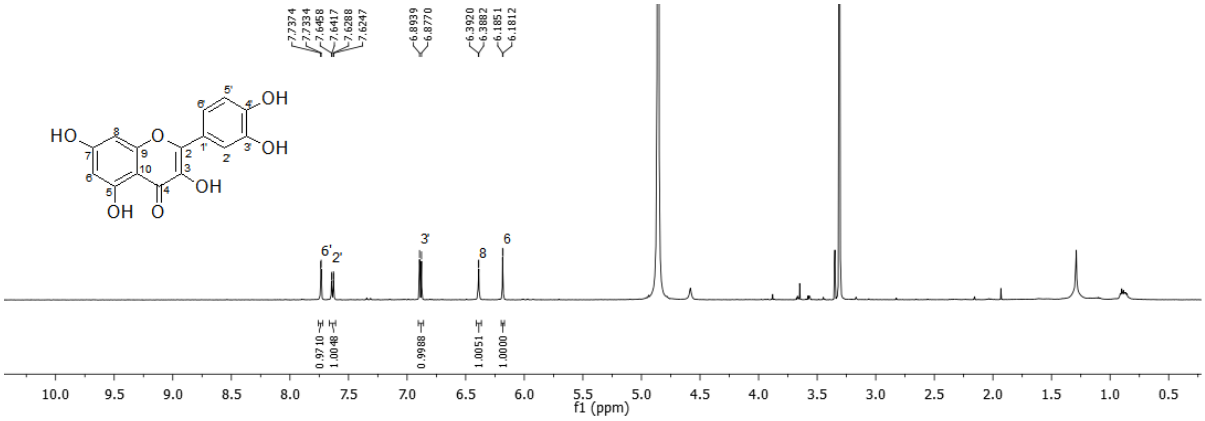

Figure S34. ^{1}H NMR spectrum of compound **10** (300 MHz, MeOD)

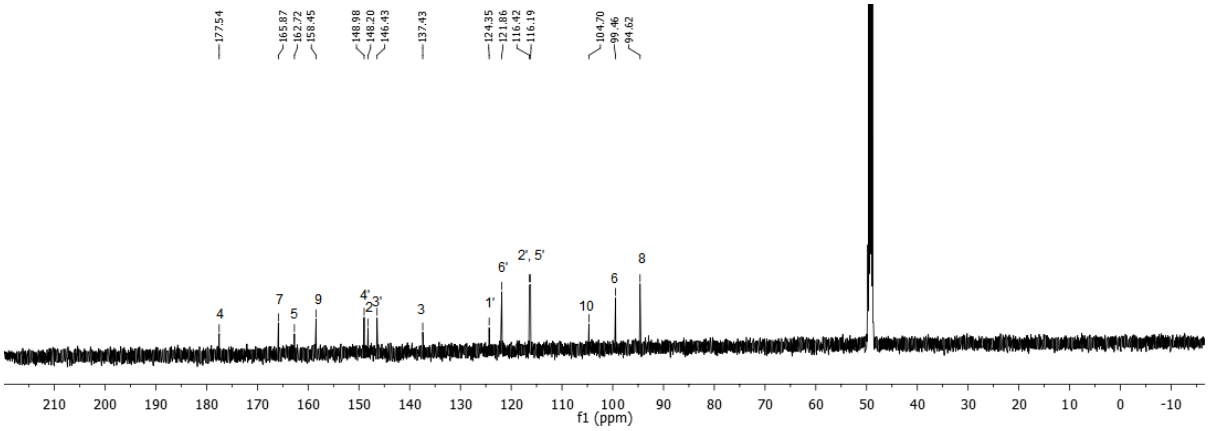

Figure S35. ^{13}C NMR spectrum of compound **10** (125 MHz, MeOD)

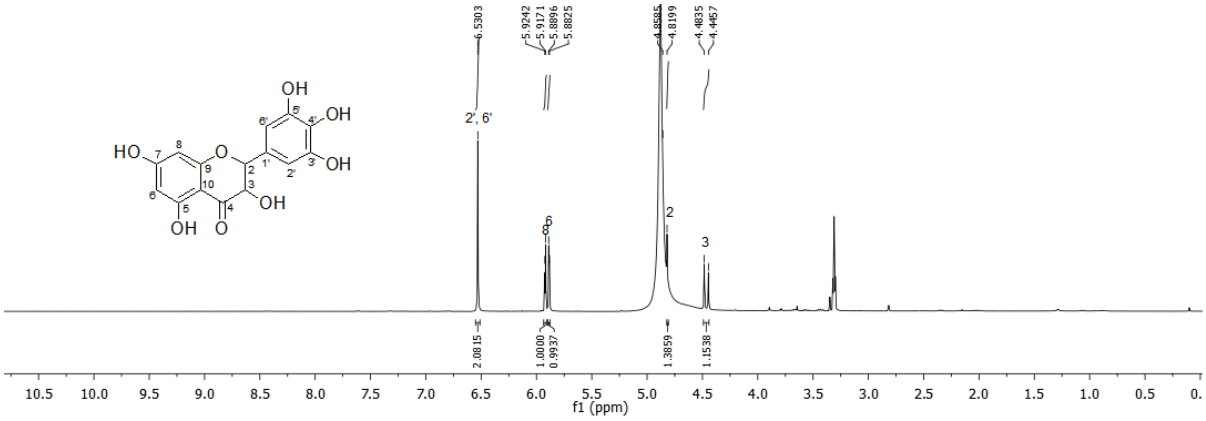

Figure S36. ^{1}H NMR spectrum of compound **11** (300 MHz, MeOD)

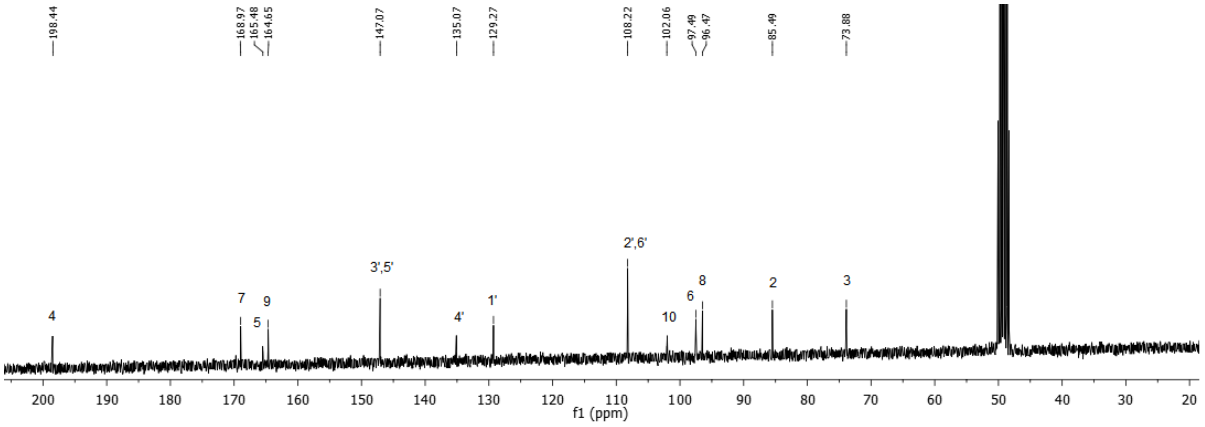

Figure S37. ^{13}C NMR spectrum of compound **11** (125 MHz, MeOD)

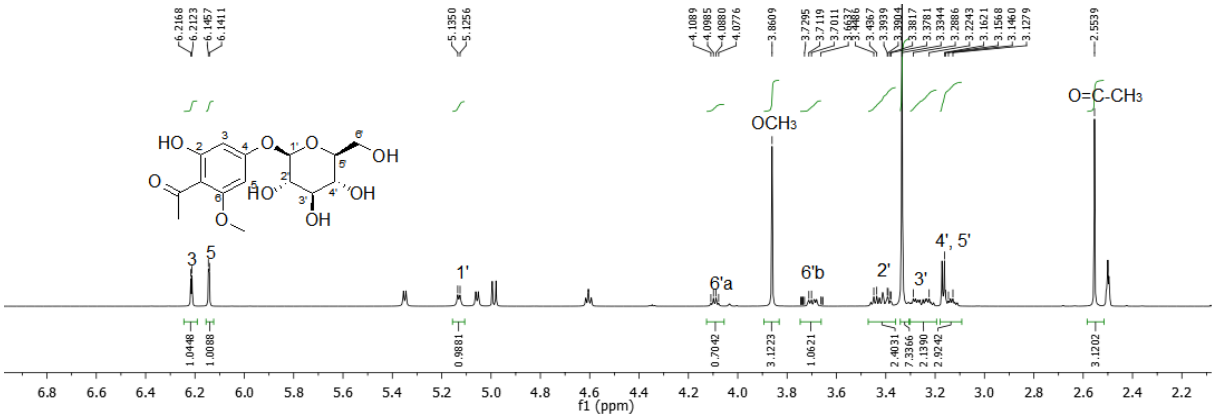

Figure S38. ^{1}H NMR spectrum of compound **12** (300 MHz, DMSO-d_6)

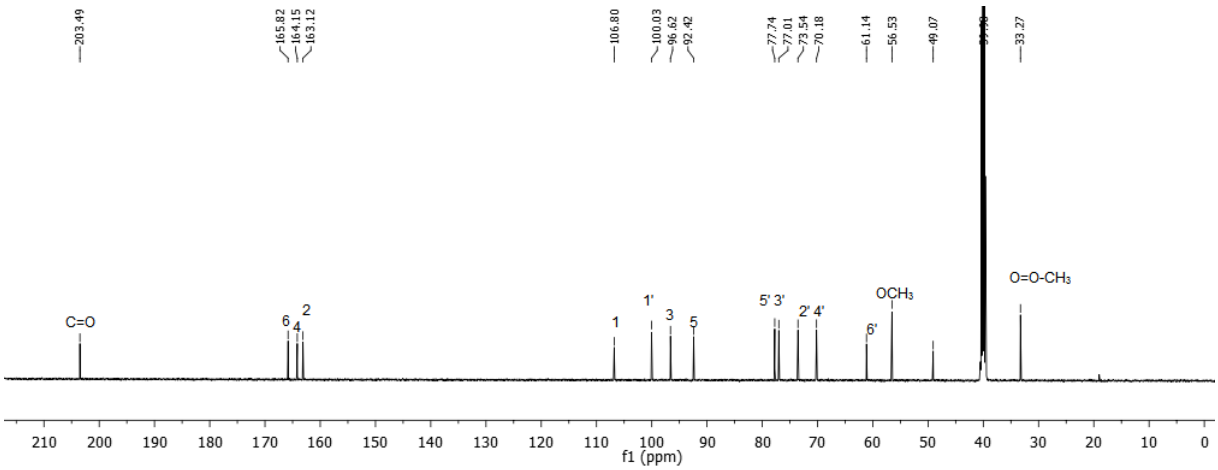

Figure S39. ^{13}C NMR spectrum of compound **12** (125 MHz, DMSO-d_6)

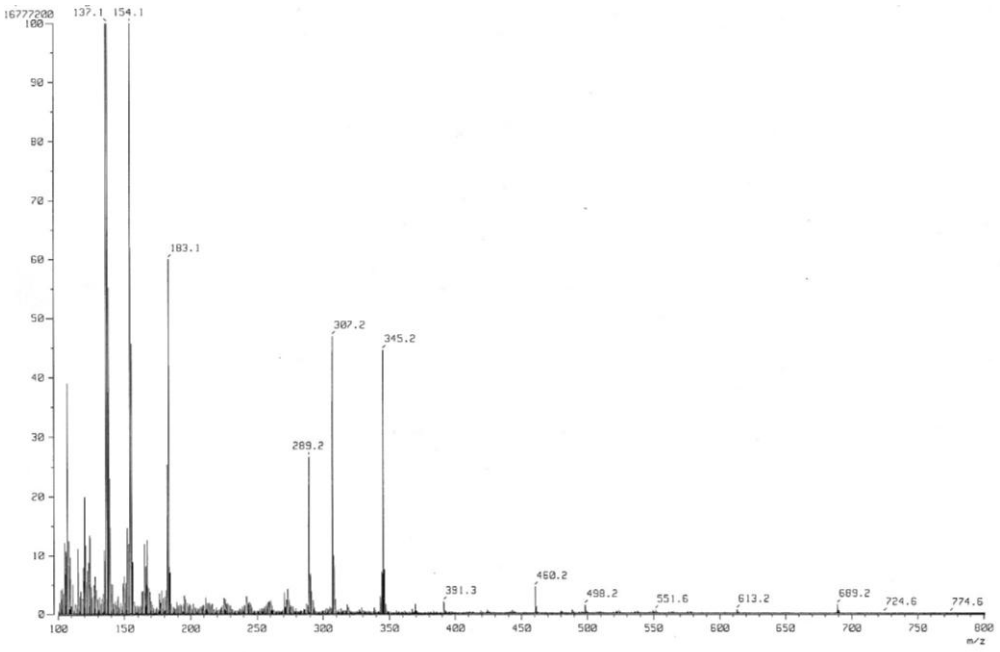

Figure S40. EIMS spectra data of compound **12.**

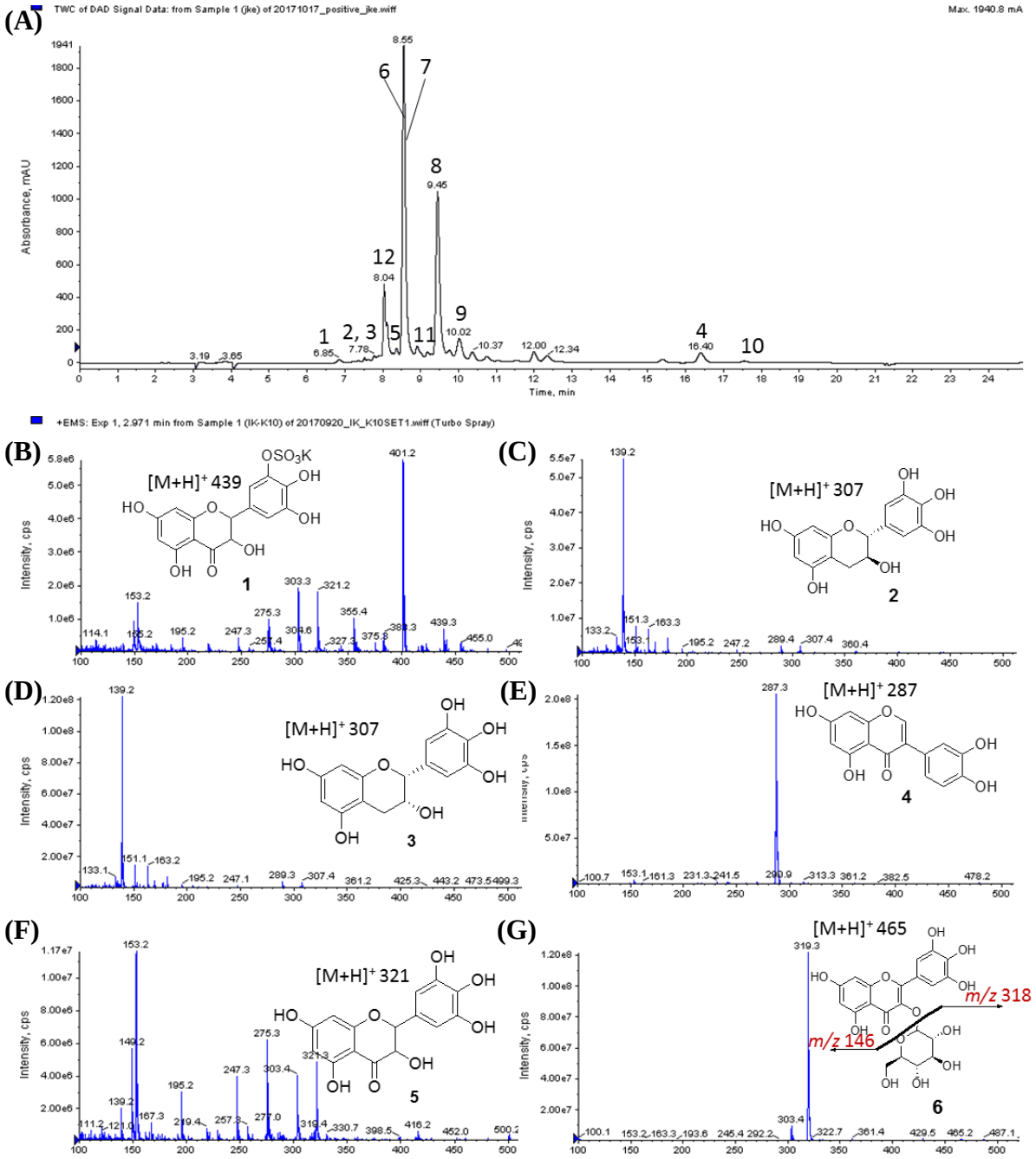
(A)
TWC of DAD Signal Data: from Sample 1 (jke) of 20171017_positive_jke.wiff
Max. 1940.8 mA
Absorbance, mAU
Time, min
1
2, 3
5
11
12
6
7
8
9
10
4
(B)
[M+H]+ 439
1
(C)
[M+H]+ 307
2
(D)
[M+H]+ 307
3
(E)
[M+H]+ 287
4
(F)
[M+H]+ 321
5
(G)
[M+H]+ 465
m/z 318
m/z 146
6
+EMS: Exp 1, 2.971 min from Sample 1 (IK-K10) of 20170920_IK_K10SET1.wiff (Turbo Spray)
Intensity, cps

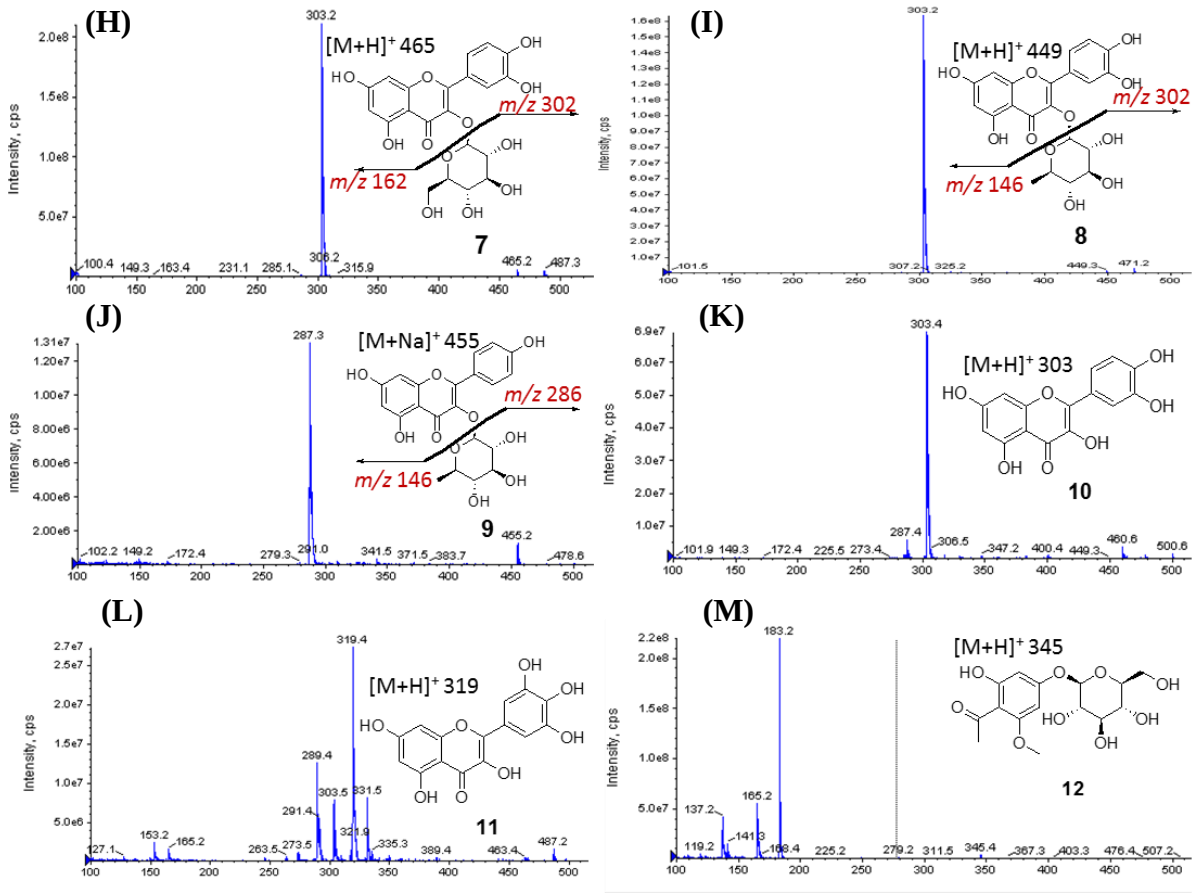

Figure S41. (A) LC-MS/MS chromatogram of *I. kaufmanniana* extract. (B-M) MS spectra of compounds **1-12**.

Table S1. Summary of antioxidant in radical scavenging experiments

Compounds	DPPH IC_{50} (μM)	·OH IC_{50} (μM)	ORAC[a] (μmol TE/g)	DNA damage protection[b] (%)
1	24.0±0.7	9.7±0.3	14.2±0.3	85.1
2	33.0±0.7	38.9±0.6	2.9±0.7	12.4
3	29.9±0.5	31.5±0.2	18.9±0.7	12.7
4	23.0±0.8	18.7±0.9	13.0±1.2	32.8
5	16.9±0.3	8.3±0.7	14.8±0.5	89.4
6	26.6±0.6	14.8±0.8	11.2±0.5	38.1
7	28.5±0.5	6.8±0.2	12.9±0.4	89.5
8	26.0±0.4	4.9±0.3	21.9±0.2	94.5
9	114.7±2.2	13.8±0.7	12.9±0.8	40.2
10	25.4±0.4	10.3±0.2	18.3±0.5	NT[d]
11	6.7±0.3	2.4±0.2	3.6±0.3	NT
12	571.1±3.5	228.7±1.8	1.7±0.1	NT
Trolox[c]	12.01±0.6	44.8±0.9	-	11.2

[a]The concentrations are the ORAC values; [b] DNA damage protections were calculated for 60 μM of compounds; [c]Trolox was used as a positive control; [d]NT is not tested.

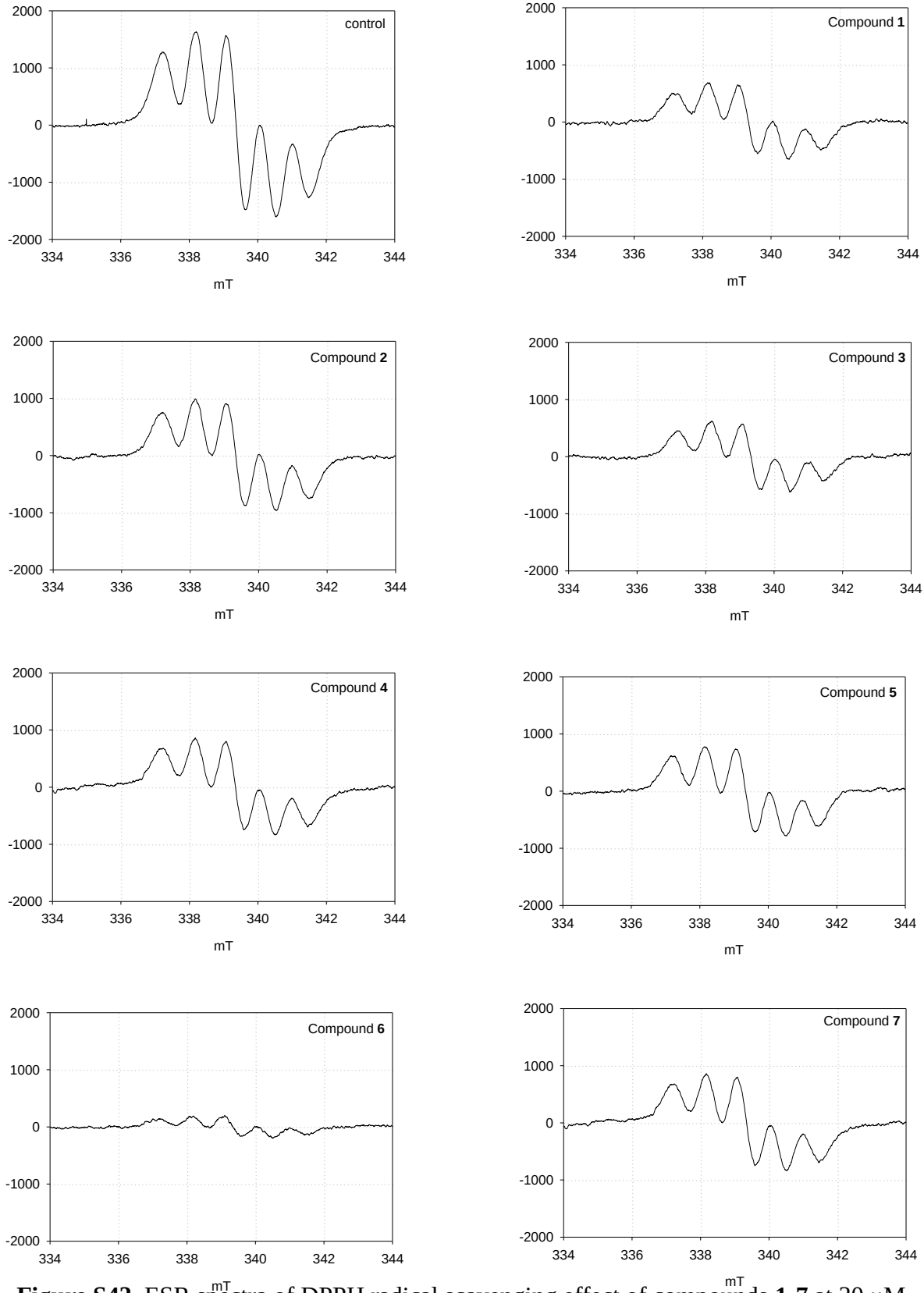

Figure S42. ESR spectra of DPPH radical scavenging effect of compounds **1**-**7** at 30 μM

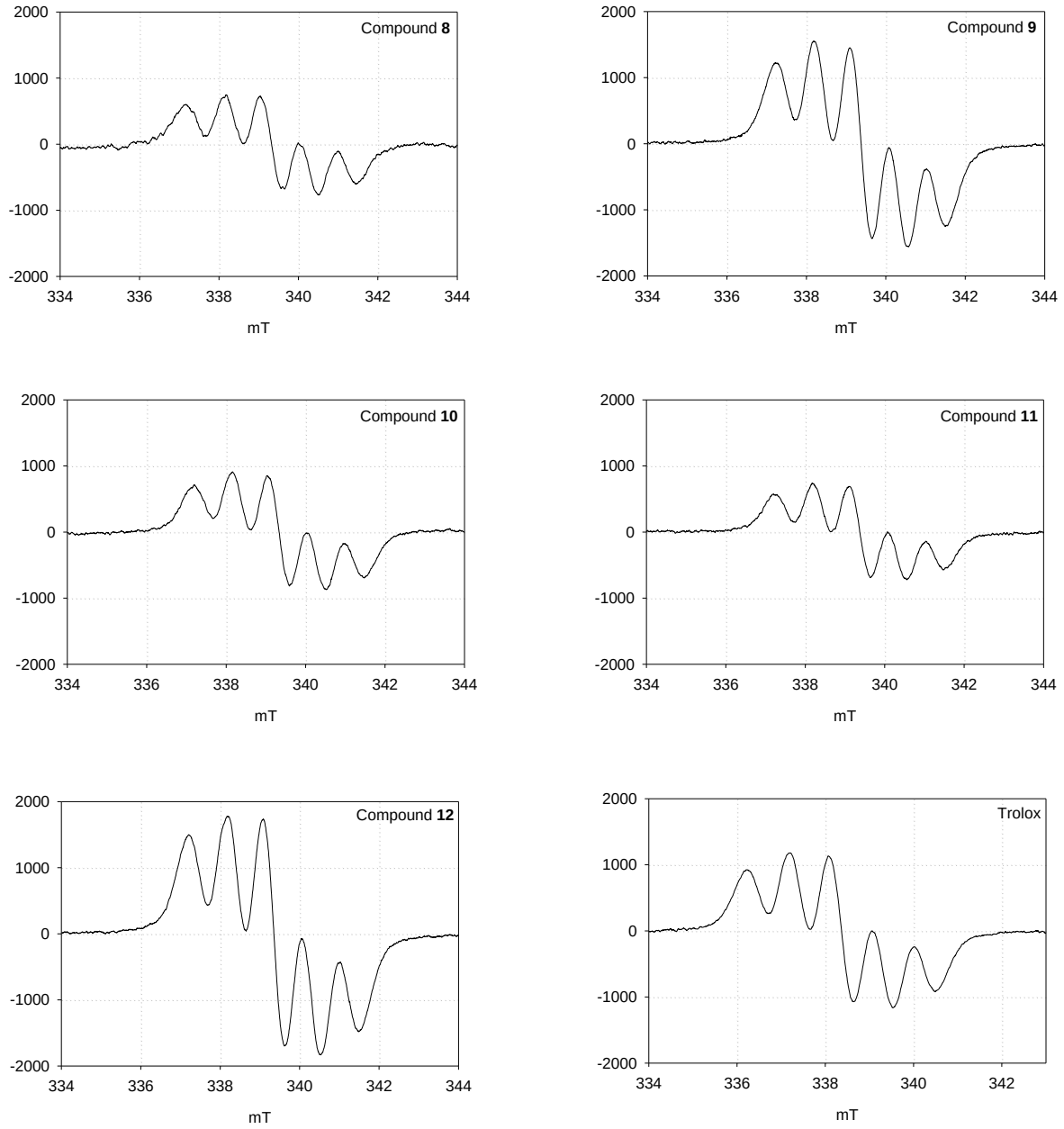

Figure S43. ESR spectra of DPPH radical scavenging effect of compounds **8**-**12**, and trolox (positive control) at 30 μM.

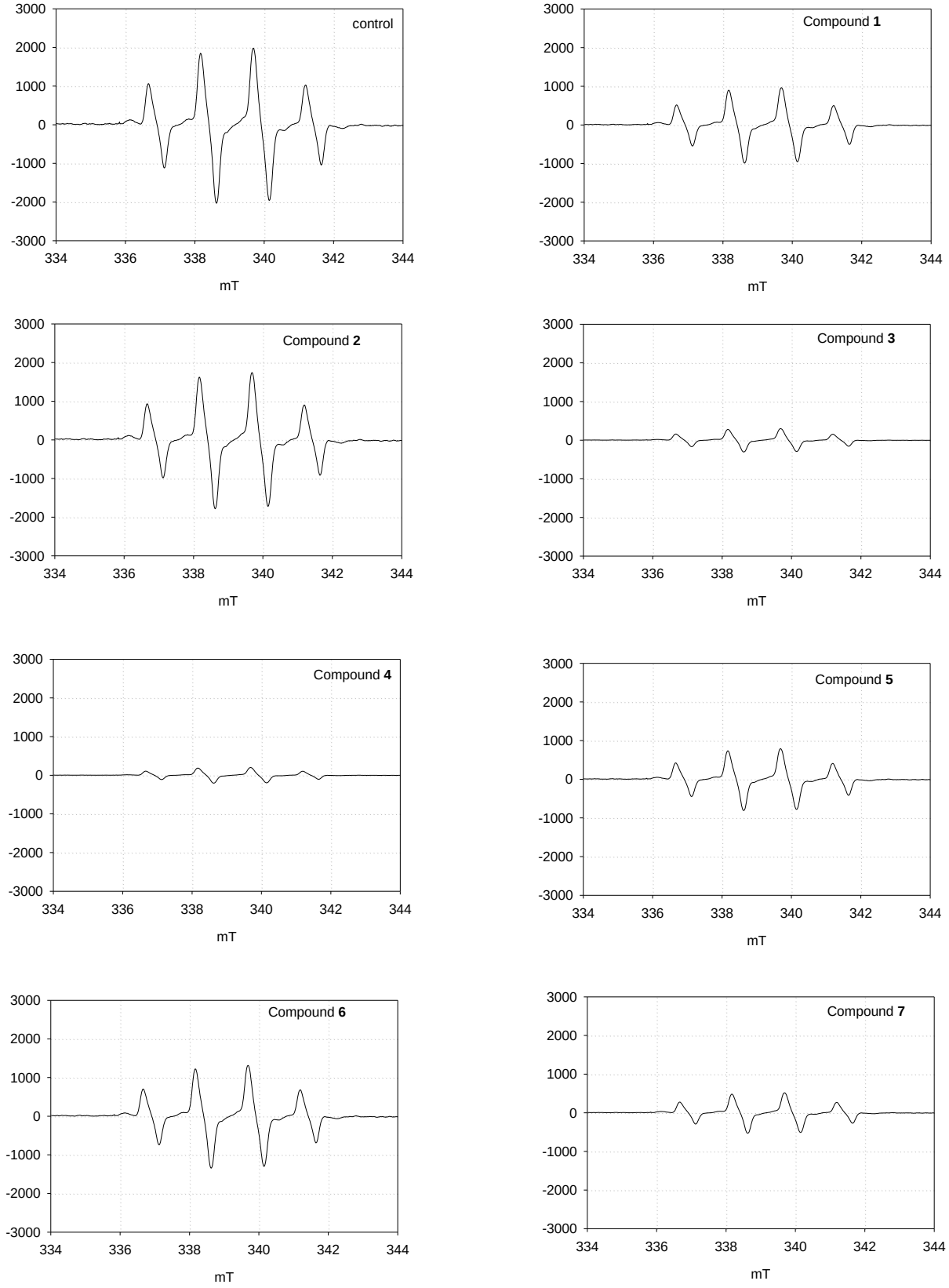

Figure S44. ESR spectra of hydroxyl radical scavenging effect of compounds**1**-**7** at 30 μM

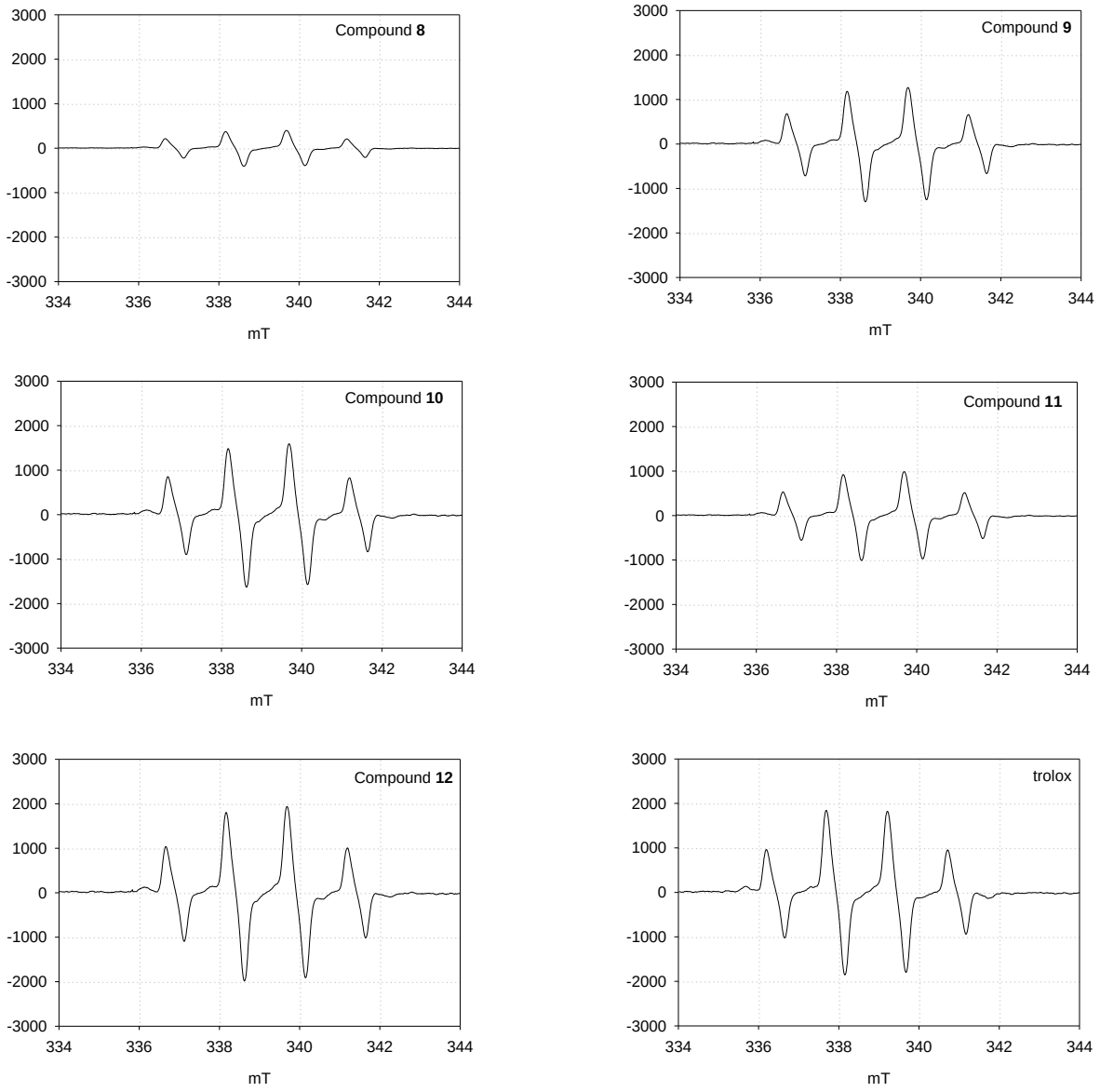

Figure S45. ESR spectra of DPPH radical scavenging effect of compounds **8**-**12**, and trolox (positive control) at 30 μM.

Table S2. pBR322 plasmid DNA protective effect of **1-9,** at 60 μM.

	scDNA band intensity	ocDNA band intensity	DNA damage (%)	DNA protective effect (%)
pBR322 DNA	100	0	-	-
Oxidative DNA	0	100	-	-
1	85.1	14.9	85.1	14.9
2	12.4	87.6	12.4	87.6
3	12.7	87.3	12.7	87.3
4	32.8	67.2	32.8	67.2
5	89.4	10.6	89.4	10.6
6	38.1	61.9	38.1	61.9
7	89.5	10.5	89.5	10.5
8	94.5	5.5	94.5	5.5
9	40.2	59.8	40.2	59.8
Trolox	11.2	88.8	11.2	88.8

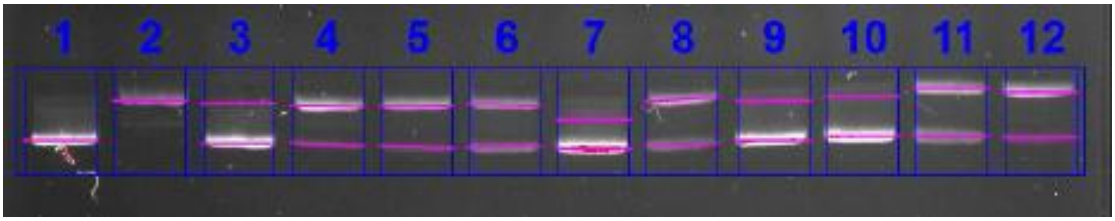

Lane 1

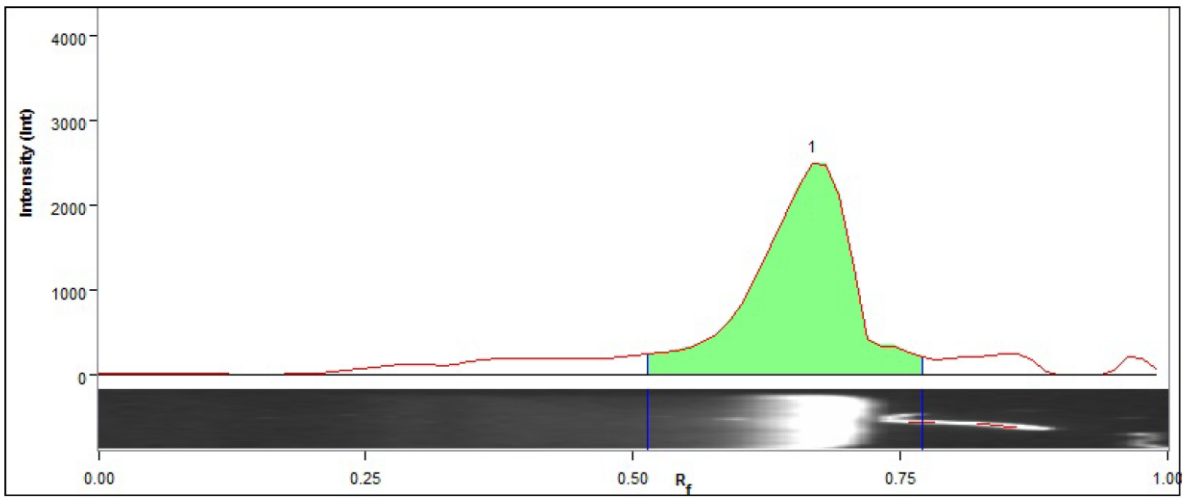

Band No.	Band Label	Mol. Wt. (KDa)	Relative Front	Volume (Int)	Abs. Quant.	Rel. Quant.	Band %	Lane %
1		N/A	0.679	1,079,557	N/A	N/A	100.0	77.2

Lane 2

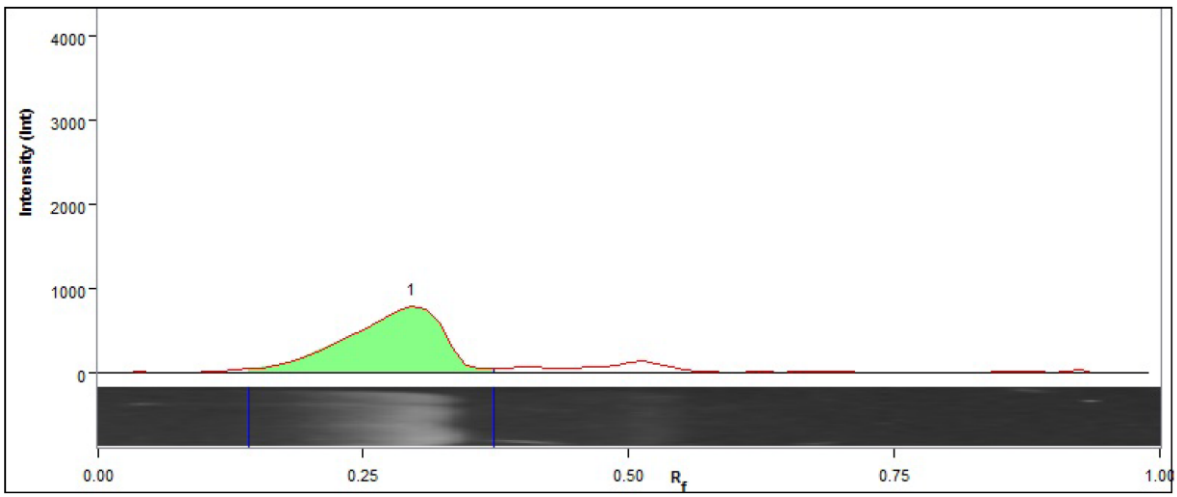

Band No.	Band Label	Mol. Wt. (KDa)	Relative Front	Volume (Int)	Abs. Quant.	Rel. Quant.	Band %	Lane %
1		N/A	0.308	345,560	N/A	N/A	100.0	81.7

Lane 3

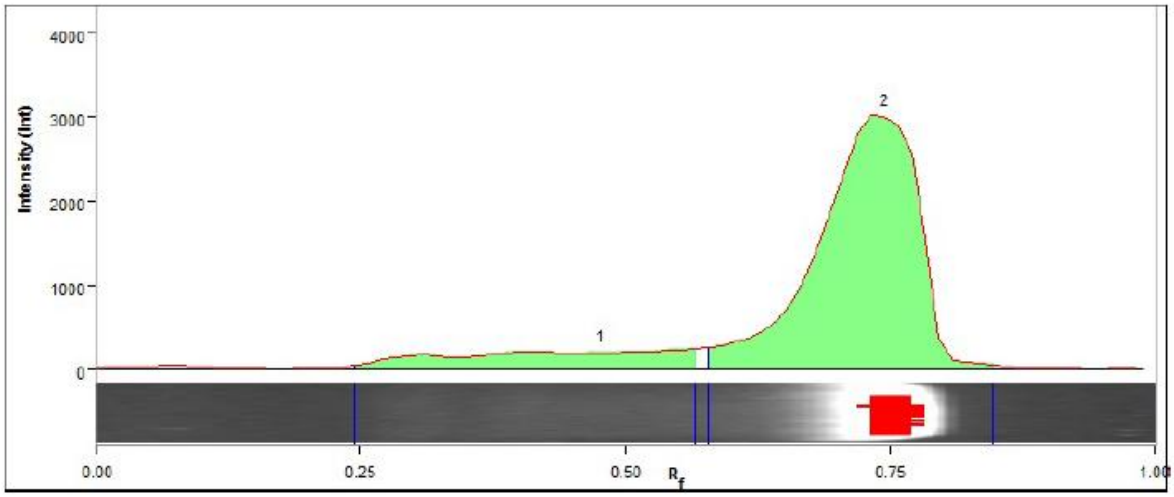

Band No.	Band Label	Mol. Wt. (KDa)	Relative Front	Volume (Int)	Abs. Quant.	Rel. Quant.	Band %	Lane %
1		N/A	0.487	243,853	N/A	N/A	14.9	14.6
2		N/A	0.756	1,397,398	N/A	N/A	85.1	83.4

Lane 4

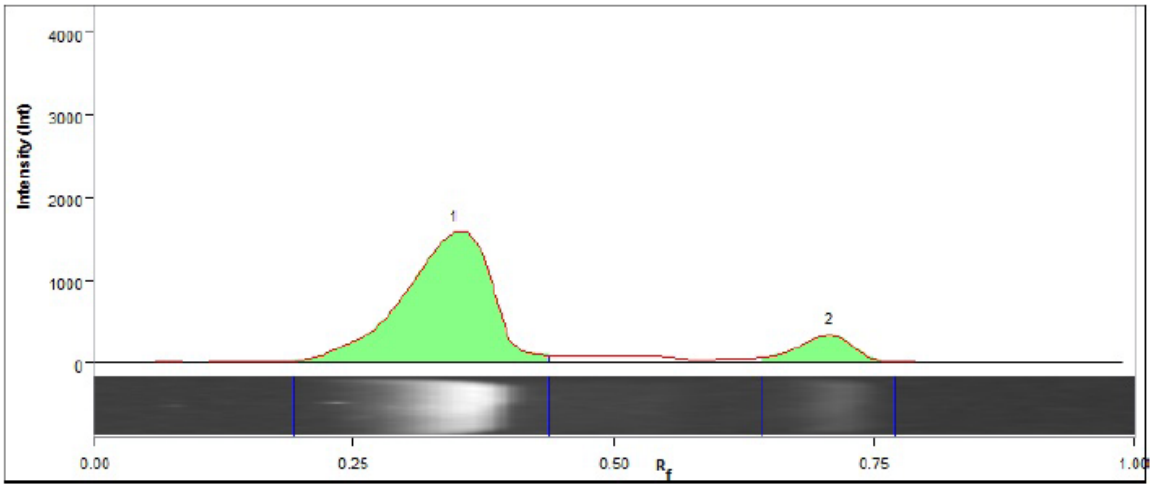

Band No.	Band Label	Mol. Wt. (KDa)	Relative Front	Volume (Int)	Abs. Quant.	Rel. Quant.	Band %	Lane %
1		N/A	0.359	649,356	N/A	N/A	87.6	80.4
2		N/A	0.718	91,849	N/A	N/A	12.4	11.4

Lane 5

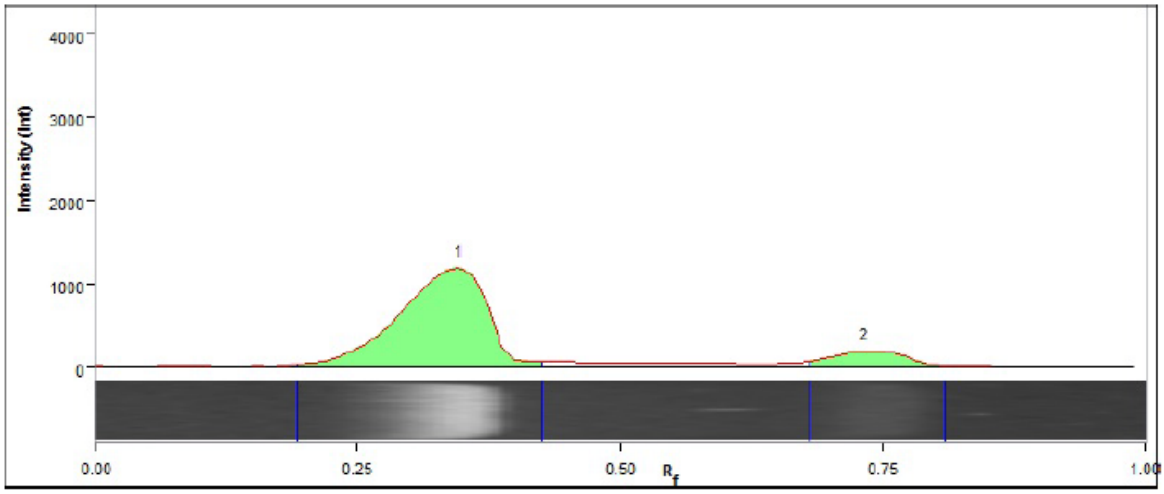

Band No.	Band Label	Mol. Wt. (KDa)	Relative Front	Volume (Int)	Abs. Quant.	Rel. Quant.	Band %	Lane %
1		N/A	0.359	479,597	N/A	N/A	87.3	78.4
2		N/A	0.744	70,013	N/A	N/A	12.7	11.4

Lane 6

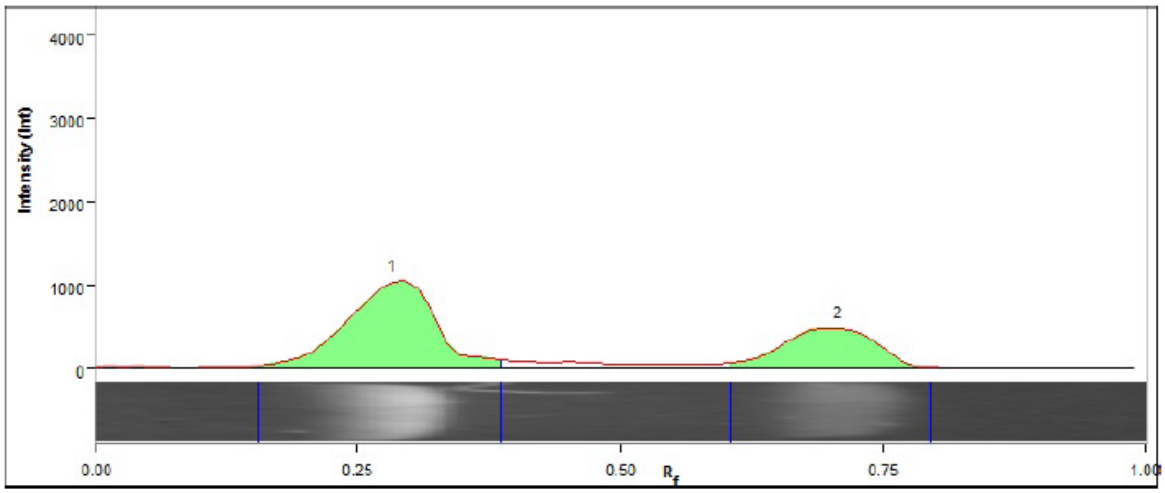

Band No.	Band Label	Mol. Wt. (KDa)	Relative Front	Volume (Int)	Abs. Quant.	Rel. Quant.	Band %	Lane %
1		N/A	0.295	437,674	N/A	N/A	67.2	61.0
2		N/A	0.718	213,749	N/A	N/A	32.8	29.8

Lane 7

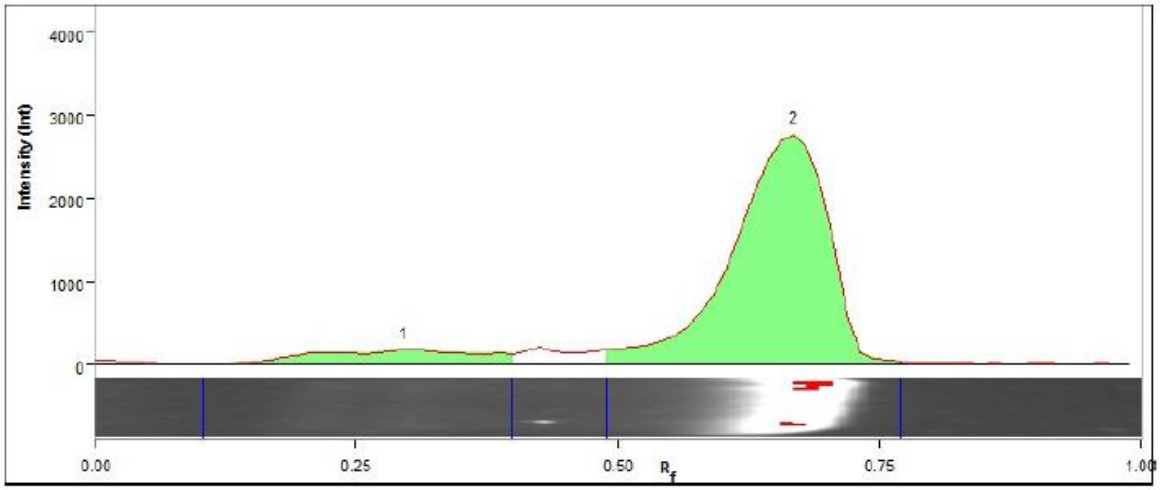

Band No.	Band Label	Mol. Wt. (KDa)	Relative Front	Volume (Int)	Abs. Quant.	Rel. Quant.	Band %	Lane %
1		N/A	0.308	147,181	N/A	N/A	10.6	10.2
2		N/A	0.679	1,236,649	N/A	N/A	89.4	85.5

Lane 8

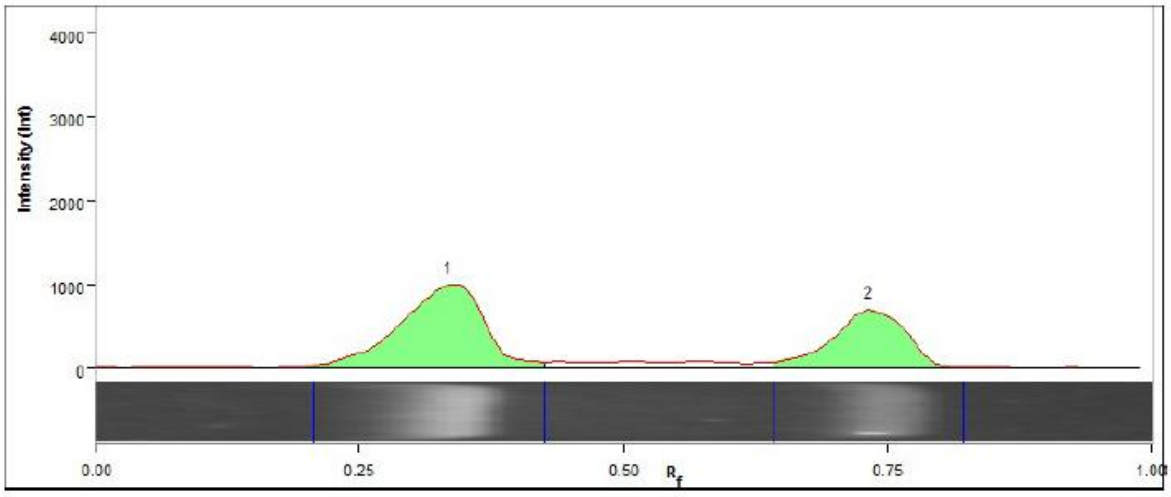

Band No.	Band Label	Mol. Wt. (KDa)	Relative Front	Volume (Int)	Abs. Quant.	Rel. Quant.	Band %	Lane %
1		N/A	0.346	385,575	N/A	N/A	61.9	54.8
2		N/A	0.744	237,493	N/A	N/A	38.1	33.7

Lane 9

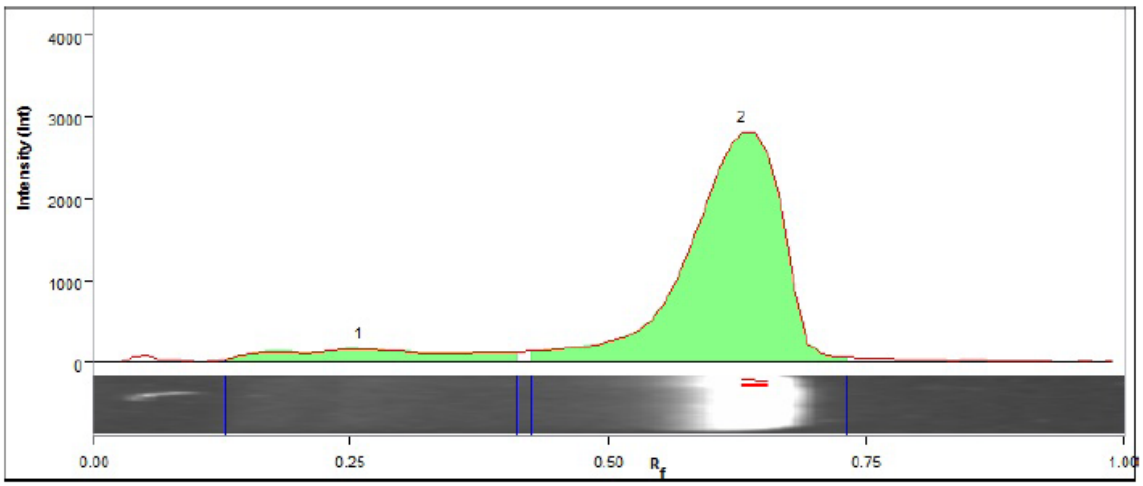

Band No.	Band Label	Mol. Wt. (KDa)	Relative Front	Volume (Int)	Abs. Quant.	Rel. Quant.	Band %	Lane %
1		N/A	0.269	148,029	N/A	N/A	10.5	10.2
2		N/A	0.641	1,258,909	N/A	N/A	89.5	87.0

Lane 10

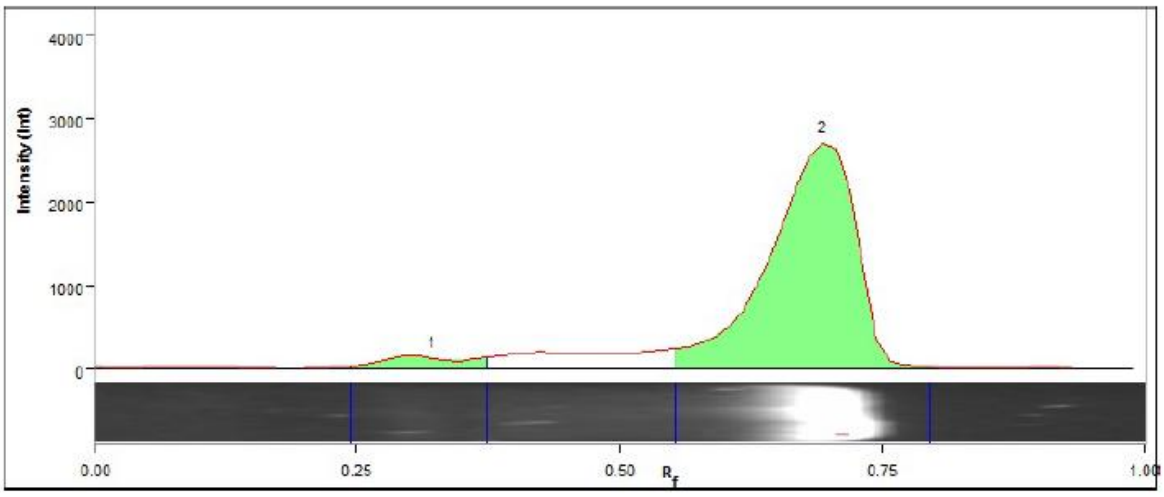

Band No.	Band Label	Mol. Wt. (KDa)	Relative Front	Volume (Int)	Abs. Quant.	Rel. Quant.	Band %	Lane %
1		N/A	0.333	62,911	N/A	N/A	5.5	4.8
2		N/A	0.705	1,087,295	N/A	N/A	94.5	82.6

Lane 11

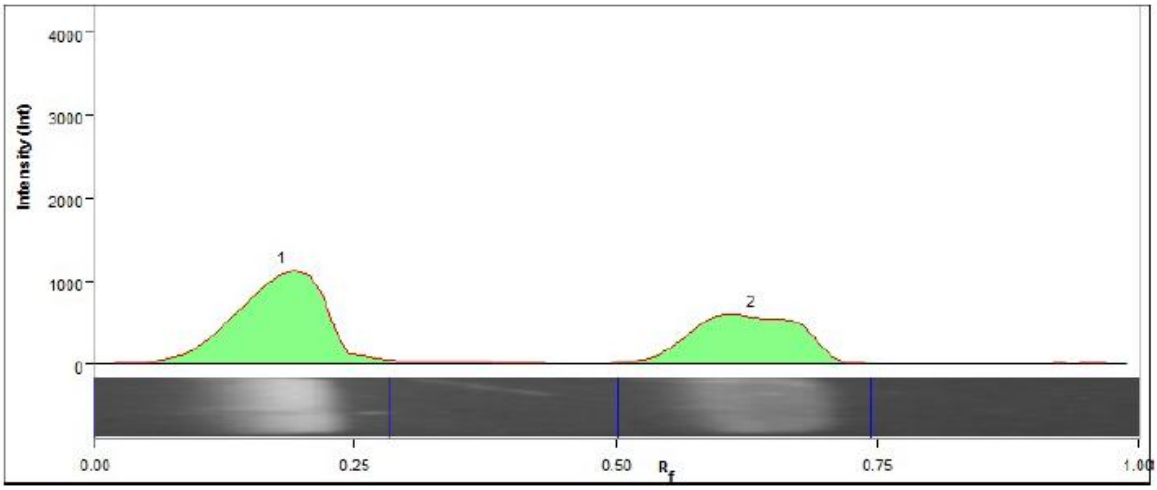

Band No.	Band Label	Mol. Wt. (KDa)	Relative Front	Volume (Int)	Abs. Quant.	Rel. Quant.	Band %	Lane %
1		N/A	0.192	471,594	N/A	N/A	59.8	58.1
2		N/A	0.641	316,940	N/A	N/A	40.2	39.0

Lane 12

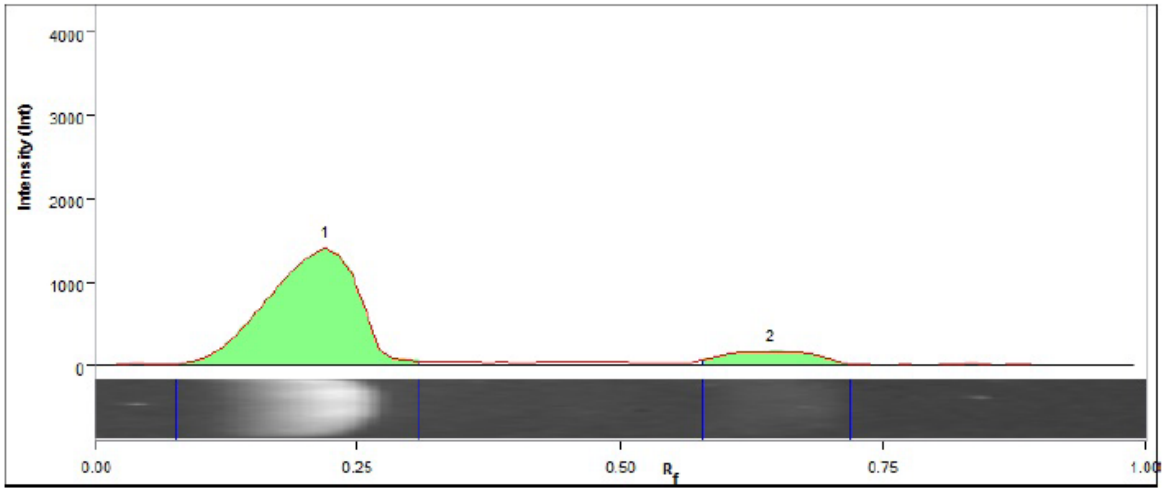

Band No.	Band Label	Mol. Wt. (KDa)	Relative Front	Volume (Int)	Abs. Quant.	Rel. Quant.	Band %	Lane %
1		N/A	0.231	591,321	N/A	N/A	88.8	81.1
2		N/A	0.654	74,677	N/A	N/A	11.2	10.2

Figure S46. Results of electrophoresis by pBR322 plasmid DNA band intensity; Lane 1, pBR322 plasmid DNA; Lane 2, oxidative DNA; Lane 3, compound **1**; Lane 4, compound **2**; Lane 5, compound **3**; Lane 6, compound **4**; Lane 7, compound **5**; Lane 8, compound **6**; Lane 9, compound **7**; Lane 10, compound **8**; Lane 11, compound **9**; Lane 12, trolox (positive

control)

Table S3. Protective effect of pBR322 plasmid DNA by dose dependent of compound **8**

	scDNA band intensity	ocDNA band intensity	DNA damage (%)	DNA protective effect (%)
pBR322 DNA	95	5	-	-
Oxidative DNA	15.3	84.7	-	-
15 mM	17.4	82.6	86.9	13.1
30 mM	32.1	67.9	71.5	28.5
60 mM	92.2	7.8	8.2	91.8
120 mM	100	0	0	100

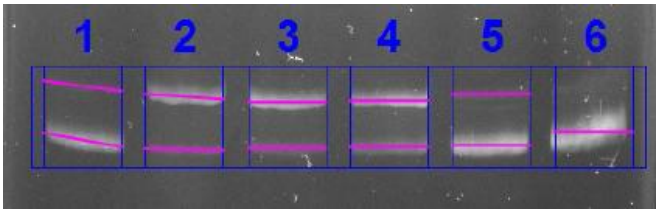

Lane 1

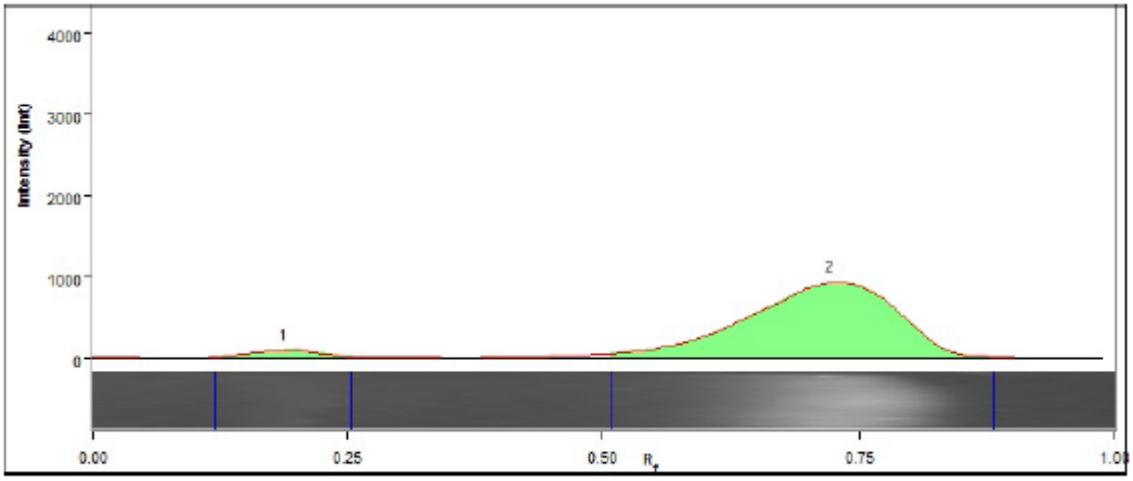

Band No.	Band Label	Mol. Wt. (KDa)	Relative Front	Volume (Int)	Abs. Quant.	Rel. Quant.	Band %	Lane %
1		N/A	0.200	36,656	N/A	N/A	5.0	4.8
2		N/A	0.733	697,566	N/A	N/A	95.0	91.8

Lane 2

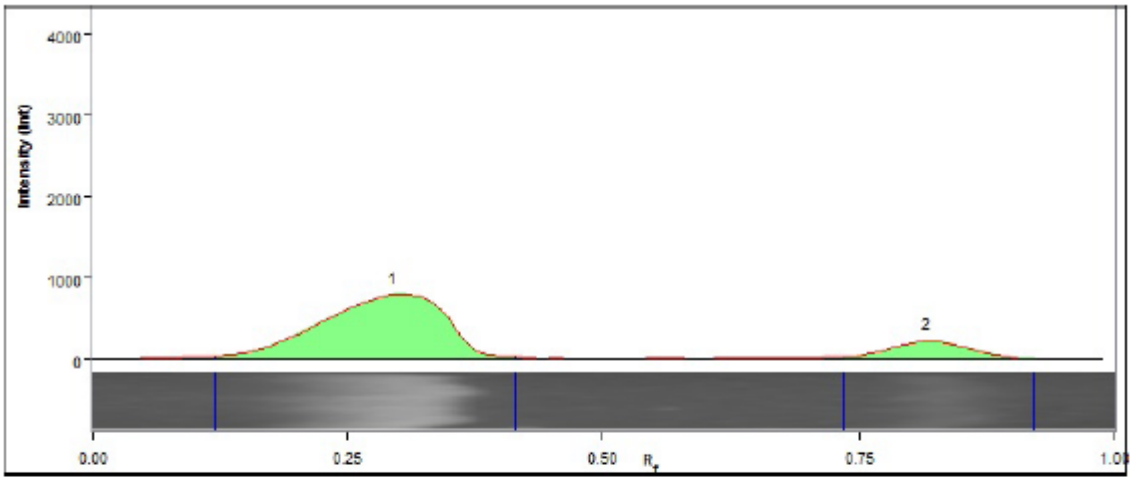

Band No.	Band Label	Mol. Wt. (KDa)	Relative Front	Volume (Int)	Abs. Quant.	Rel. Quant.	Band %	Lane %
1		N/A	0.307	493,522	N/A	N/A	84.7	81.3
2		N/A	0.827	89,262	N/A	N/A	15.3	14.7

Lane 3

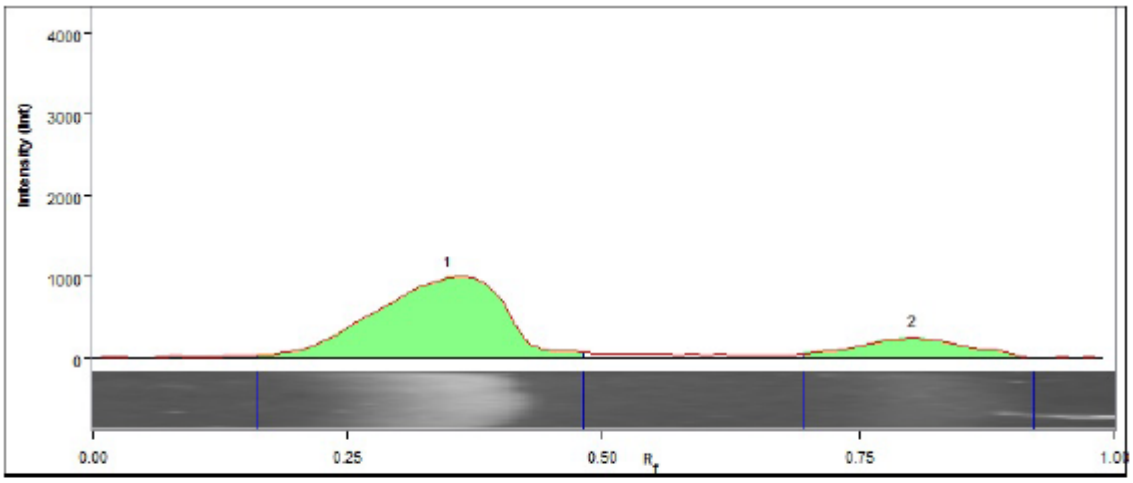

Band No.	Band Label	Mol. Wt. (KDa)	Relative Front	Volume (Int)	Abs. Quant.	Rel. Quant.	Band %	Lane %
1		N/A	0.360	650,528	N/A	N/A	82.6	77.4
2		N/A	0.813	136,880	N/A	N/A	17.4	16.3

Lane 4

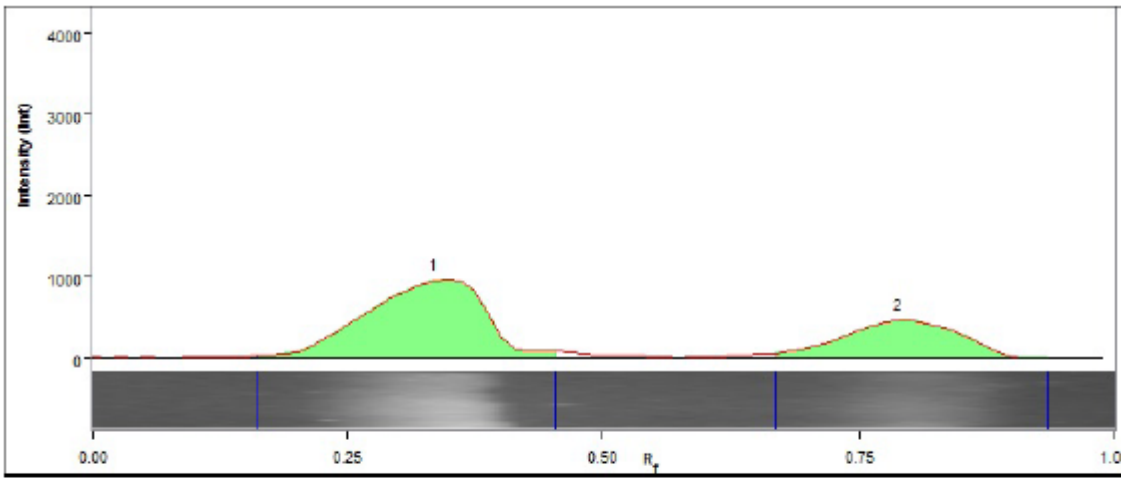

Band No.	Band Label	Mol. Wt. (KDa)	Relative Front	Volume (Int)	Abs. Quant.	Rel. Quant.	Band %	Lane %
1		N/A	0.347	576,462	N/A	N/A	67.9	65.2
2		N/A	0.800	272,078	N/A	N/A	32.1	30.8

Lane 5

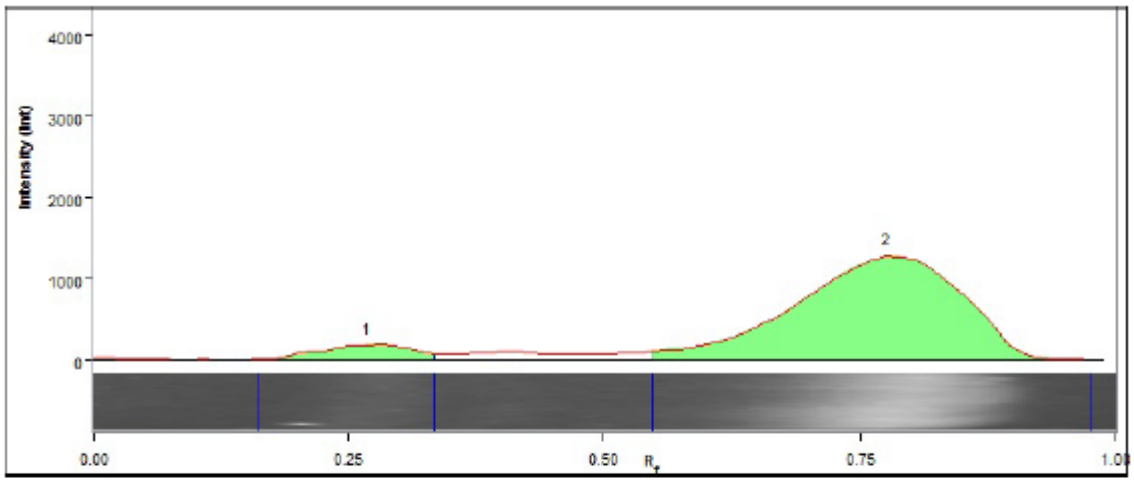

Band No.	Band Label	Mol. Wt. (KDa)	Relative Front	Volume (Int)	Abs. Quant.	Rel. Quant.	Band %	Lane %
1		N/A	0.280	89,668	N/A	N/A	7.8	7.3
2		N/A	0.787	1,058,384	N/A	N/A	92.2	86.2

Lane 6

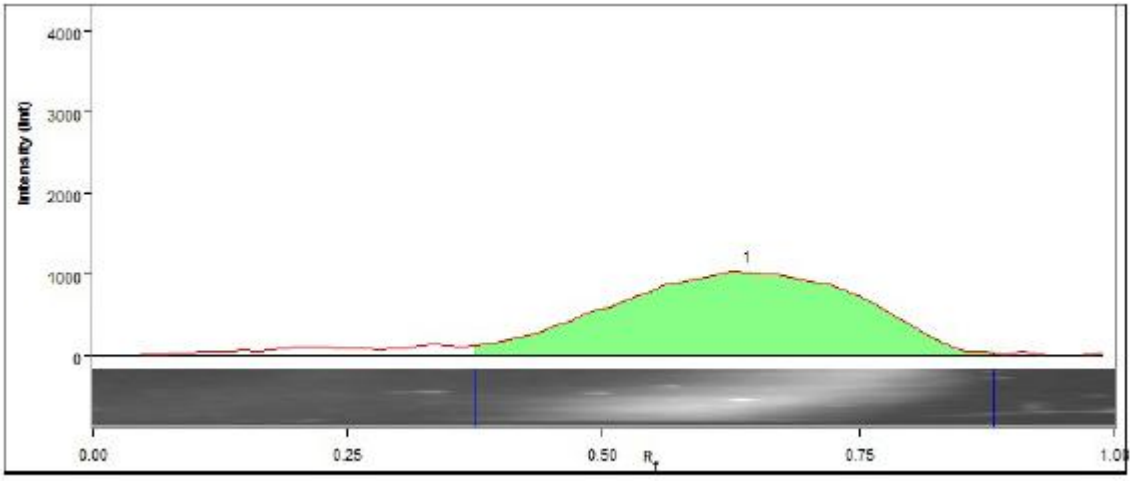

Band No.	Band Label	Mol. Wt. (KDa)	Relative Front	Volume (Int)	Abs. Quant.	Rel. Quant.	Band %	Lane %
1		N/A	0.653	1,314,164	N/A	N/A	100.0	91.9

Figure S47. Results of electrophoresis by pBR322 plasmid DNA band intensity against dose-dependent with compound **8**; Lane 1, pBR322 plasmid DNA; Lane 2, oxidative DNA; Lane 3, 15 mM; Lane 4, 30 mM; Lane 5, 60 mM; Lane 6, 120 mM.

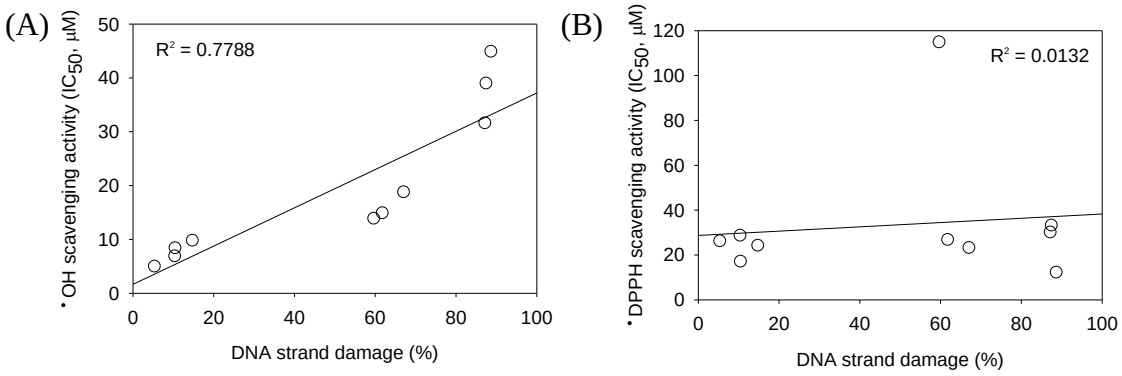

Figure S48. (A) Correlation between DNA damage and hydroxyl radical. (B) Correlation between DNA damage and DPPH radical.

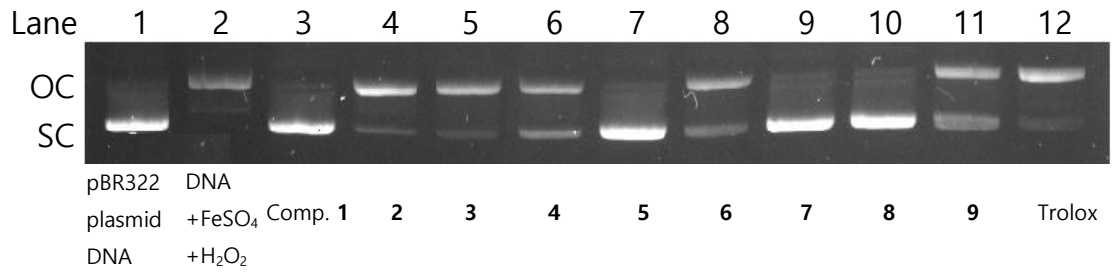

Figure 49S. Protective effect of the best-performing metabolites at 60 μM against DNA damage induced by Fenton's reaction.

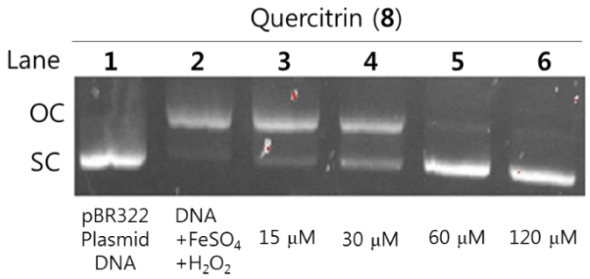

Figure 50S. Dose-dependent protective effect of quercitrin (**8**) against DNA damage.

References

Chen CY, Hsieh SL, Hsieh MM, Hsieh SF, Hsieh TJ. 2004. Substituent chemical shift of rhamnosides from the stems of Cinnamomum osmophleum. Chinese Pharm J. 56:141–146.

David JM, Cruz FG, Guedes MLS, Cháve JP. 1996. Flavonol glycosides from Davilla flexuosa. J Braz Chem Soc.

Davis AL, Cai Y, Davies AP, Lewis JR. 1996. 1H and13C NMR Assignments of Some Green Tea Polyphenols. Magn Reson Chem. 34:887–890. http://doi.wiley.com/10.1002/%28SICI%291097-458X%28199611%2934%3A11%3C887%3A%3AAID-OMR995%3E3.0.CO%3B2-U

Fanie B, Heerden V, Brandt EV. 1980. Synthesis of the Pyranoisoflavonoid, Heminitidulan. lsoflavanoid and Rotenoid Glycosides from the Bark of Daibergia nitidda Welw. ex Bak. JCS Perkin I. 9:2463.

Gadetskaya AV., Tarawneh AH, Zhusupova GE, Gemejiyeva NG, Cantrell CL, Cutler SJ, Ross SA. 2015. Sulfated phenolic compounds from Limonium caspium: Isolation, structural elucidation, and biological evaluation. Fitoterapia. 104:80–85. https://linkinghub. elsevier.com/retrieve/pii/S0367326X15300125

Ishiguro K, Nagata S, Fukumoto H, Yamaki M, Takagi S, Isoi K. 1991. A flavanonol rhamnoside from Hypericum japonicum. Phytochemistry. 30:3152–3153. http://linkinghub.elsevier.com/retrieve/pii/S0031942200982773

Kim HH, Oh MH, Park KJ, Heo JH, Lee MW. 2014. Anti-inflammatory activity of sulfate-containing phenolic compounds isolated from the leaves of Myrica rubra. Fitoterapia.

Kim J, Wang Y, Song Y, Uddin Z, Li Z, Ban Y, Park K. 2018. Antioxidant Activities of Phenolic Metabolites from Flemingia philippinensis Merr. et Rolfe and Their Application to DNA Damage Protection. Molecules. 23:816. http://www.mdpi.com/1420-3049/23/4/816

Matsuda H, Morikawa T, Xu F, Ninomiya K, Yoshikawa M. 2004. New Isoflavones and Pterocarpane with Hepatoprotective Activity from the Stems of Erycibe expansa. Planta Med. 70:1201–1209. http://www.thieme-connect.de/DOI/DOI?10.1055/s-2004-835852

Nonaka G-I, Muta M, Nishioka I. 1983. Myricatin, a galloyl flavanonol sulfate and prodelphinidin gallates from Myrica rubra. Phytochemistry. 22:237–241.: http://linkinghub.elsevier.com/retrieve/pii/S0031942200800977

Pereira C. 2012. Flavonoids and a neolignan glucoside from Guarea macrophylla. Quim Nov. 35:1123–1126.

Prasad D. 1999. A new aromatic glycoside from the roots of Prunus armeniaca. Fitoterapia.

Sai V, Chaturvedula P, Huang R. 2013. Isolation and NMR Spectral Studies of Dihydromyricetin. J Pharmacogn Phytochem JPP. 113:113–115.